The Role of Chronic Inflammation in Lung Tumorigenesis and the Identification of Potential Biomarkers for Lung Cancer Treatment

by

Chia-Hsin Liu

MD, National Defense Medical Center, Taiwan, 2006

Submitted to the Graduate Faculty of

the Department of Environmental and Occupational Health

Graduate School of Public Health in partial fulfillment

of the requirements for the degree of

Doctor of Philosophy

University of Pittsburgh

2019

UNIVERSITY OF PITTSBURGH

GRADUATE SCHOOL OF PUBLIC HEALTH

This dissertation was presented

by

Chia-Hsin Liu

It was defended on

July 18, 2019

and approved by

Bruce R. Pitt, PhD, Professor
Department of Environmental and Occupational Health
Graduate School of Public Health, University of Pittsburgh

Phouthone Keohavong, PhD, Associate Professor
Department of Environmental and Occupational Health
Graduate School of Public Health, University of Pittsburgh

Binfeng Lu, PhD, Associate Professor
Department of Immunology
School of Medicine, University of Pittsburgh

Dissertation Advisor: YuanPu Peter Di, PhD, Associate Professor
Department of Environmental and Occupational Health
Graduate School of Public Health, University of Pittsburgh

YuanPu Peter Di, PhD

The Role of Chronic Inflammation in Lung Tumorigenesis and the Identification of Potential Biomarkers for Lung Cancer Treatment

Chia-Hsin Liu, PhD

University of Pittsburgh, 2019

Abstract

Lung cancer is a significant public health concern as the leading cancer-related deaths in the United States. Chronic inflammation is strongly involved in the pathogenesis of chronic obstructive pulmonary disease (COPD) and increases the risk of lung cancer. The inflammatory responses in the tumor microenvironment not only promote tumor progression but also have effects on treatment efficacy such as immunotherapy. In addition, Metalloproteinases (MMPs), which increase expression in COPD have been reported to correlate with tumor recurrence in surgically resected non-small cell lung cancer.

In the first study, we used the cigarette smoke carcinogen 4-(methylnitrosamino)-1-(3-pyridyl)-1-butanone (NNK) to generate genetic instability and parallelly provided repeated LPS to induce chronic lung inflammation. This novel exposure paradigm creates an immunosuppressive microenvironment favorable of tumor progression similar to that of inflammation-associated lung tumorigenesis in patients. Furthermore, the model was used to evaluate the efficacy of anti-PD-1 immunotherapy as well as myeloid-derived suppressor cells depletion on lung tumorigenesis. In addition, we identified immune gene signatures, which predict treatment responses and survival outcome of patients with NSCLC treated with either PD-1 blockade or conventional therapies.

In the second study, we conducted transcriptome analysis of lung adenocarcinoma cases in two discovery cohorts and discovered metalloproteinases (MMPs)-enriched gene clusters, which contained MMPs and related genes. We further identified a MMPs-gene signature from the two MMPs-gene clusters, which predicted recurrence and worse overall survival in patients with stage I lung adenocarcinoma after surgical resection. The high MMPs-gene signature expression remained an independent risk factor after adjusting covariates and showed enrichment in KRAS-mutant lung tumors. Finally, the MMPs-gene signature was successfully validated in an independent cohort. The MMPs-gene signature is a potential prognostic biomarker to stratify patients with stage I lung adenocarcinoma into subgroups based on their risk of recurrence for aiding physicians to decide the use of adjuvant therapeutics.

For public health significance, our study provided a clinically-relevant lung cancer animal model in elucidating the effects of chronic inflammation on lung tumorigenesis and the efficacy of cancer therapies. The utility of gene signatures in predicting lung cancer treatment and survival could be useful for personalized therapeutics.

Table of Contents

List of Tables

List of Figures

Acknowledgment

I would like to thank my graduate advisor Dr. Peter Di for his great support and insightful guidance to my studies and projects in PhD training and my road on becoming an independent researcher. I would also like to thank my committee members, Dr. Bruce Pitt, Dr. Phouthone Keohavong, and Dr. Binfeng Lu for their critical suggestions on my projects. I would also like to thank all the co-authors for their efforts and contributions.

None of the work contained in this thesis was done alone. I would like to thank Dr. Zhong Chen for the experimental suggestions and academic discussion on these projects. I would also like to thank all lab members and classmates for their direct or indirect help.

Most importantly, I would like to thank my parents and family members for their endless love and support.

1.0 Introduction

1.1 Lung Cancer Overview

Lung cancer is the leading cancer-related deaths in the United States with estimated 228,150 newly diagnosed cases and 142,670 deaths in 2019 (1). About 85% of lung cancer is non-small cell lung cancer (NSCLC), of which lung adenocarcinoma and lung squamous cell carcinoma are the most common histological subtypes (2). Tobacco smoking is the most common etiology for lung cancer and accounts for most lung cancer-related deaths (3-6). Occupational exposure to agents such as arsenic, chromium, asbestos, nickel, cadmium, beryllium, silica, and diesel fumes are known to cause lung cancer (7-9). In addition, other possible risk factors include acquired lung diseases (eg, COPD), infections, family history of lung cancer, and Radon gas seem to cause lung cancer (4). Regardless of the identification of well-established causal risk factors, cigarette smoking remains the primary risk factor of the global epidemic of lung cancer.

Although a significant amount of effort has been made for lung cancer in regards to screening, minimally invasive techniques for diagnosis, and advancement in therapeutics, the 5-year survival rate remains low at only 18% (1). The majority of patients is diagnosed as locally advanced or metastatic disease, which the curative surgery is no longer feasible (10). Regardless of curative surgery for early-stage lung cancer, 20% to 40% of stage I patients will have tumor recurrence, which remains the main causes of cancer-related death (11-14). Patients with stage I lung adenocarcinoma, which is the most common histological subtype, vary in survival outcome. It indicates that the current tumor (T), node (N), metastasis (M) staging system fails to distinguish patients with a higher risk of recurrence for the stage I disease following surgical resection (15).

Adjuvant chemotherapy has been shown to decrease disease recurrence and prolonged overall survival in patients with stage II-III disease (16-19), but its role in stage I remains controversial and lacks biomarkers for the indication of treatments. In addition, most patients with advanced or metastatic disease are typically treated with cytotoxic chemotherapy with a modest increase in survival. During the last two decades, the discovery of small molecular inhibitors targeting genetic alternations has improved the survival rates for the subsets of cancer patients. Patients with the mutated epidermal growth factor receptor (EGFR) responded to erlotinib or gefitinib, and those with altered anaplastic lymphoma receptor tyrosine kinase genes (ALK) responded to crizotinib (20, 21). A study showed that the frequency of *EGFR*, and *ALK* mutation in lung adenocarcinoma is 27% and <8%, respectively that the majority of lung cancer patients either don't contain these genetic alternations (22). Even though the subsets of patients with these mutations treated with targeted therapies, they eventually developed resistance within 1-2 years of starting therapy (23). Immunotherapy such as immune checkpoint blockade (ICB) has been used recently for lung cancer treatment with promising clinical responses, but the response rate is low and only a small subset of patients benefited from the treatment (24). While most patients who responded to initial ICB treatment, they finally develop resistance. Several mechanisms for acquired resistance to ICBs have been identified including the defects in interferon-γsignaling or major histocompatibility complex presentation, and the increased levels of the enzyme indoleamine 2,3-dioxygenase (IDO1), which impaired T cell function by the deprivation of tryptophan (25-27).

Overall, major challenges still remain in lung cancer treatment, including the need of reliable biomarkers to stratify stage I NSCLC with high risk of recurrence for adjuvant therapies, better understanding of mechanisms of resistance to targeted therapy to allow them to be prevented

or overcome, the better predictors of responses to immunotherapy, and new drugs and rationally designed drug combination therapies for advanced stage NSCLC.

1.2 Chronic Inflammation Correlates with Lung Tumorigenesis

Inflammation is an essential process for host immune responses to prevent pathogen invasion and also involves in wound healing. However, persistent and uncontrolled inflammatory responses are associated with active recruitment of inflammatory cells and the production of mediators such as cytokines, chemokines, growth factors, and matrix-degrading enzymes leading to inflammatory microenvironment (28). It has been reported that "smoldering" inflammation in the tumor microenvironment has many tumor-promoting effects such as tumor-cell migration, invasion, and metastasis, epithelial-mesenchymal transition and angiogenesis (29). In addition, chronic inflammation also induces immunosuppressive mechanism associated with accumulation of suppressive cells like myeloid-derived suppressor cells (MDSCs) and regulatory T cells (Tregs) as well as the increased immunosuppressive mediators such as IL-10 and TGF-β, which help tumors escape from immune surveillance (30, 31). Although the exact mechanisms of inflammation in promoting lung cancer remain unclear, two connected hypotheses have been proposed that an intrinsic pathway driven by genetic alternations leads to neoplasia and inflammation, and an extrinsic pathway driven by inflammatory conditions increases cancer risk (29).

1.2.1 Inflammation links COPD and lung cancer

Cigarette smoking is the leading causes of chronic obstructive pulmonary disease (COPD) and lung cancer, accounting for the third leading cause of death in the United States and the leading cause of cancer death worldwide, respectively (32, 33). Several epidemiological studies have shown that patients with COPD have a higher incidence of lung cancer risk than those without obstructive lung disease (34). In addition, COPD is characterized by chronic airway inflammation and has an increased risk of lung cancer independent of cigarette smoking, which suggests the further link between inflammation and lung cancer (35, 36). The bacterial colonization by *Pseudomonas aeruginosa* is frequently found in COPD and associated with increased airway inflammation and acute exacerbations (37, 38). Lipopolysaccharide (LPS) is a major component of the outer cell wall of Gram-negative bacteria and may involve in bacterial infection-induced exacerbations of COPD, which contributes to the progression of the disease (39). However, the mechanism of bacteria associated with chronic inflammation, especially those induced by LPS in lung carcinogenesis remains unclear.

1.2.2 COPD-related inflammation is associated with immunotherapy responses

There is increasing evidence for the role of local immune responses and systematic inflammation in the progression of tumors, which has an influence on the efficacy of treatments (40). Immunotherapy such as checkpoint inhibition has emerged as a new treatment modality in lung cancer and showed durable clinical responses (41, 42). However, the overall treatment response rate for non-small cell lung cancer (NSCLC) is around 15-20%, that only a minority of patients are benefited from the treatment, due to the lack of clear biomarkers or indications for the

responders or non-responders (24). Two recent studies showed increased survival in PD-1 blockade recipients of NSCLC patients with COPD, suggesting that COPD-related dysregulated inflammation affects PD-1 blockade efficacy (43, 44). However, the mechanism of the effective immunotherapy remains unclear in NSCLC, and the immunological biomarkers used in the clinics just partially predicted the lung cancer patients' responding rates. This leaves a big gap for the current diagnosis and prognosis of lung cancer patients under immunotherapy (45).

1.2.3 Immune gene signatures predict immunotherapy efficacy

The development of specific gene expression profiling for a subset of tumors provided the possibility to identify prognostic gene expression signatures and patient selection for targeted therapies. The immune gene signatures recently identified include the genes of cell surface markers, cytokines and chemokines, cellular signaling molecules, and transcription factors, which is indicative of the presence of specific immune-related responses (46). The modulation of immune contexture of tumor microenvironment holds the potential in cancer treatment. For instance, the baseline T cell-inflamed tumor microenvironment is associated with checkpoint inhibitors and adaptive cell therapy (47, 48). In agreement, multiple immune-related gene signatures have been reported to correlate with clinical responses in a subset of patients with solid tumors treated with checkpoint inhibitors (47, 49-51). However, the complete immune gene signature, which is associated with enhanced therapeutic and survival benefits in lung cancer patients and related animal models have not been clearly identified.

1.2.4 MMPs overexpressed in COPD and associated with early-stage lung cancer recurrence

The emphysematous component of COPD is characterized by the excessive inflammatory responses with the destruction of matrix destruction, and confer to an increased risk of lung cancer (34). The matrix metalloproteinases (MMPs) are a family of 24 proteolytic enzymes, which can degrade the extracellular matrix (52). Several MMPs such as MMP1, MMP9, and MMP12, which are cable of degrading elastin and collagen have been implicated in the pathogenesis of COPD in response to cigarette smoke (53-55). In addition, many of these enzymes are reputed to promote lung tumor growth in many phases of cancer progression, including invasiveness, angiogenesis, and metastasis (56-58).

Tumor recurrence remains the leading cancer-related deaths in patients with early-stage lung cancer after curative surgery. Several MMPs such as MMP2, MMP9, MMP10, and MMP12 have been reported to correlate with recurrence in surgically resected early-stage NSCLC (59-61). However, these MMPs-based biomarker studies showed inconsistent or not reproducible results in different cohorts, which limit the use as prognostic markers for clinical application (62). In addition, and their effects on survival outcome for patients with stage I lung adenocarcinoma after curative surgery remains unknown.

1.3 Dissertation Objectives

In the first study, we plan to address the role of chronic inflammation, especially induced by LPS, in lung tumorigenesis. We hypothesize that LPS-mediated chronic inflammation alters

immune contexture in the tumor microenvironment contributing to lung carcinogenesis and affecting immunotherapy efficacy. Therefore, we first developed a two-staged lung cancer mouse model, which mimics the smoking carcinogen-induced, and COPD-related airway inflammation promoted lung cancers. To further explore the effects of inflammation on immunotherapy responses, the mice exposed to NNK or NNK/LPS were treated with either IgG control or anti-PD-1. In addition, anti-Ly6G was administrated to evaluate the impact of the MDSCs depletion on lung tumorigenesis. Furthermore, we analyzed the published lung cancer datasets to identify potential immune gene signature in predicting immunotherapy efficacy.

In the second study, we hypothesize that multiple MMPs were co-expressed and increased expression in lung adenocarcinomas and correlated with worse survival outcome. We sought to characterize the expression of MMPs and related genes by analyzing transcriptome data of lung adenocarcinoma cases. We aimed to develop an MMPs-related gene signature as a prognostic molecular marker to stratify patients with stage I lung adenocarcinoma into subgroups based on the risk of recurrence for aiding physicians to decide the personalized adjuvant therapeutics.

2.0 Materials and Methods

2.1 Murine Model and Reagents

FVB/NJ (7 weeks, female) mice were purchased from Jackson Laboratory (Bar Harbor, Maine, USA). Procedures were approved by the Institutional Animal Use and Care Committee of the University of Pittsburgh. Lipopolysaccharides from Pseudomonas aeruginosa (L8643, Sigma, St Louis, MO) was resuspended and diluted in phosphate-buffered saline (PBS). NNK (M325750, Toronto Research Chemicals) was resuspended in methanol and diluted in PBS. Mice were treated with PBS, 3mg i.p. NNK (biweekly for 4 weeks), 5µg LPS by intranasal instillation (weekly for 16 weeks), or combined NNK and LPS (Figure 1A) as previously described (63). In addition, mice exposed to NNK with/without 10-week LPS instillation were treated with 200µg i.p. IgG2a, (2A3, BioXCell, West Lebanon, NH), 200µg i.p. anti-PD-1 (RMP1-14, BioXCell) for 6 weeks (Figure 6A) or combined NNK and 16-week LPS exposure mice were treated with 200µg i.p. IgG2a, anti-PD-1, anti-Ly6G (1A8, BioXCell) or in combination (Figure 6D). Mice were euthanized one week after the last treatment, and samples were obtained for transcript, protein, histopathological, and immunohistochemical analyses.

2.2 Immune Gene Signature Analysis

The normalized mRNA of 730 immune-related genes and patient profiles were downloaded from GSE93157 cohort (51). Tumor samples from 22 non-squamous (Non-SqNSCLC) and 13

squamous non-small cell lung cancer (SqNSCLC) before anti-PD-1 treatment were analyzed. The tumor response to anti-PD-1 treatment was classified as nonprogressive disease (NPD) including stable disease (SD), partial response (PR), complete response (CR) and progression disease (PD) based on modified RECIST 1.1 criteria. Differentially expressed genes (n=130, absolute fold change >1.5 and unadjusted P <0.05) between NPD and PD were determined using Partek Genomic Suite and assigned as immune gene panel. Immune cell gene signatures for T-, B-, and NK-cell were defined by the genes, which were present in two or more studies of eight published signatures (46, 64-70). IL17 and IL22 were selected as the Th17 cell signature (71). The median gene level from the signature was used for the expressional level quantification. The mouse ortholog of immune signature transcripts was used for murine model gene signature analysis.

2.3 The Cancer Genome Atlas (TCGA) Data Analysis

TCGA lung adenocarcinoma RNAseq and clinical data (n=517) were obtained from UCSC Xena (http://xena.ucsc.edu/). The immune gene panel (n=117 with low expression genes with mean <1 filtered out), were used for signature analysis. In survival analysis, the stratification of signature as high or low depends on the expression level with the best separation of survival curves among subgroups.

2.4 Histopathology, Immunohistochemistry, and Immunofluorescence Analysis

Mouse lung lobes were fixed with 4% paraformaldehyde (Affymetrix), embedded in paraffin and evaluated by H&E staining, immunohistochemistry (IHC), or immunofluorescence (IF) staining. Antibodies used for immunostaining (all from Cell Signaling) included PD-L1 (DV53B, 1:100), PD-1 (D7D5W, 1:200), CD4 (D7D2Z, 1:400), CD8 (D4W1Z, 1:400). Digital images of H&E staining and IHC slides were obtained at 40× magnification (0.23 μm per pixel) using a whole-slide scanner (Hamamatsu nanozoomer HT 2.0) for tumor area quantification. Tumor area was quantified by the percentage of tumor area divided by the total lung area using ImageJ Software. Lung tumor grade was classified by criteria previously published (72). Multiplex tissue IF staining was performed with Opal staining system (PerkinElmer, MA), and images were captured using Nikon 90i microscope with 4′,6-diamidino-2-phenylindole for nuclear staining. Quantification of positively stained cells was performed using NIS-Elements Microscope Imaging Software. For tumor-infiltrating T lymphocytes characterization in the tumor microenvironment, the number of CD4 and CD8 T cells infiltrating to tumors was taken and the density of cell (number/mm2) was calculated based on tumor area. In addition, the percentage of PD-1 co-localization with CD4 or CD8 was also calculated.

2.5 Western Blot Analysis

Lung-protein extracts from mouse tissue were separated by SDS-PAGE under reduced conditions and transferred onto a PVDF membrane (Millipore). The membranes were immunoblotted overnight at 4°C with anti-PD-L1 (AF1019, R＆D, 0.5μg/ml). Antibody binding

was detected with SuperSignal West Pico PLUS Chemiluminescent Substrate according to the manufacturer's instructions (ThermoFisher Scientific).

2.6 Flow Cytometry

Cells isolated from tumor-bearing lungs were processed for surface labeling with several antibody panels staining for CD4, CD8, CD11b, and Ly6-G markers. Fc receptors were blocked using Fc-Block (BD Biosciences). Cells were further permeabilized using Transcription Factor Buffer Set (BD Biosciences) and stained for IFN-γ, IL-17, and Foxp3. Data were acquired using the FACSAria flow cytometer and analyzed using FlowJo software (Treestar).

2.7 Mouse mRNA Microarray Analysis

RNA extraction was performed using Trizol method (Sigma). RNA purity and integrity of samples were assessed by Bioanalyzer. The cDNA synthesis and hybridization onto HD Whole Mouse Genome Microarray (Agilent, G2519F-014868). Partek Genomics Suite 7 (Partek, St. Louis, MO) was used to process the raw microarray data, and RMA method was used for background correction. Differential expression analysis between NNK/LPS and NNK was performed using Partek Genomics Suite, and Benjamini–Hochberg method was used to adjust the raw *P* values for multiple testing. Only genes with fold change (up- and down-regulated) >2 and false discovery rate (FDR) <0.05 were considered as differentially expressed genes (DEGs).

Hierarchical clustering heatmap was conducted using Partek Genomics Suite. Data are deposited in the Gene Expression Omnibus database (submitted).

2.8 Ingenuity Pathway Analysis of NNK/LPS vs NNK DEGs (IPA)

List of DEGs between NNK/LPS and NNK, which contains 1179 genes was used to carry out gene set enrichment analysis using Ingenuity pathway analysis (IPA, http://www.ingenuity.com). IPA was used to determine which pathways were differentially represented in the identified significant genes, compared to the Ingenuity knowledge base.

2.9 Quantitative RT-PCR

Total cellular RNA was extracted by Trizol method (Sigma) and reverse-transcribed by random primers using High Capacity cDNA Reverse Transcriptase Kit (ThermoFisher Scientific). The reverse transcription reaction was then subjected to PCR amplification using Fast SYBR Green Master Mix (ThermoFisher Scientific). PCR signals were recorded on ABI 7900HT Fast Real-Time PCR and the data was normalized by mouse 18s ribosomal RNA analyzed by RQ Manager Software. Primer sets included *Pdcd1*, *Ctla4*, *Lag3*, and *Tim3*. All primer sequences are in the supplementary data.

2.10 Cytokine Quantification in Bronchoalveolar Lavage Fluid and Lung-Protein Extracts

The levels of proinflammatory mediators in bronchoalveolar lavage fluid (BALF) were quantified using magnetic bead 10-plex MILLIPLEX MAP Kit (Millipore, USA). In addition, the concentration of interferon gamma (IFN-γ) in lung-protein extracts were measured by enzyme-linked immunosorbent assay (ELISA) (R&D Systems, USA). These assays were performed according to the manufacturer's instructions. The results were expressed in the BALF samples as pg/ml, and lung lysates normalized to the total protein concentration as pg/ml/mg.

2.11 Patient and Expression Data

2.11.1 GSE31210 cohort

The microarray expression data and clinical data were previously obtained under an IRB approved protocol, with informed consents and download from the National

Center for Biotechnology Information Gene Expression Omnibus database (http://www.ncbi.nlm.nih.gov/geo) (73). Raw gene-expression data were normalized by MAS5. A total of 226 lung adenocarcinoma cases consisting of 168 stage I and 58 stage II cases and 20 normal lung tissue were subjected to expression profiling. The 204 cases who received complete resection with free resection margins and no involvement of mediastinal lymph nodes and did not receive postoperative chemotherapy and/or radiotherapy, unless relapsed, were subjected to survival analyses. 22 cases were excluded for prognosis analysis due to incomplete resection or adjuvant therapy.

2.11.2 TCGA cohort

TCGA lung adenocarcinoma RNAseq and clinical data were obtained under IRB approved protocols with informed consents and downloaded from UCSC Xena (http://xena.ucsc.edu/). A total of 517 lung adenocarcinoma cases and 59 adjacent lung tissue were subjected to expression profiling. Among the 517 cases including 277 stage I cases who have survival data were subjected to survival analysis.

2.11.3 GSE30219 cohort

The microarray expression data and clinical data were previously obtained under an IRB approved protocol, with informed consents and download from the National

Center for Biotechnology Information Gene Expression Omnibus database (http://www.ncbi.nlm.nih.gov/geo) (74). Raw gene-expression data were normalized by robust multi-array average (RMA). A total of 70 stage I (T1N0M0) lung adenocarcinoma cases who received surgery and did not receive postoperative chemotherapy and/or radiotherapy selected from 293 lung cancer cases was subjected for survival analysis.

2.12 Ingenuity Pathway Analysis of MMPs (IPA)

MMP-related gene clusters and signature including 150-gene cluster, 185-gene cluster, and 36-gene MMP signature were used to carry out gene set enrichment analysis using Ingenuity pathway analysis (IPA, http://www. ingenuity.com). IPA was used to determine which pathways

were differentially represented in the identified significant genes, compared to the Ingenuity knowledge base.

2.13 Gene Set Enrichment Analysis (GSEA)

GSEA was applied using ranked lists of genes from GSE31210 cohort based on mutation status and sorted by Signal2Noise. After Kolmogorov-Smirnoff testing, 36-gene MMP signature showing a $P < 0.05$ were considered enriched between mutation status under comparison.

2.14 Bioinformatic and Statistical Analysis

A two-tailed Student's *t*-test was used for two group comparisons, and ANOVA was used for comparisons of three or more groups. Differential expression analysis between tumor and normal lung tissue was performed using Partek Genomics Suite (Partek, St. Louis, MO), and Benjamini–Hochberg method was used to adjust the raw *P* values for multiple testing. Only genes with fold change (up- and down-regulated) >2.5 and FDR <0.05 were considered as differentially expressed genes (DEGs). Hierarchical clustering heatmap was conducted using Partek Genomics Suite. Survival was compared using Kaplan-Meyer analysis. The stratification of signature as high or low depends on the expression level with significant differences in the survival outcomes and the lowest log-rank *P* value among subgroups. The log-rank test was used to compare survival or event-free survival between groups, and Cox proportional hazards modeling was used for

univariate and multivariate analyses. Chi-squared test was used to compare frequencies in one or more categories. $P<0.05$ was considered significant.

3.0 Inflammation Promotes Tobacco Carcinogen-Induced Lung Cancer and Determines Immunotherapy Efficacy

3.1 Introduction

Smoking is a well-established risk factor for lung cancer and the main cause of COPD (75). COPD is characterized by chronic lung inflammation, and patients with COPD have increased risks for lung cancer after controlling for smoking (76, 77). This suggests that COPD is an independent risk factor of lung cancer and provides the further link between inflammation and lung cancer. Bacterial colonization by Pseudomonas aeruginosa is frequently found in COPD and correlates with increased inflammation and acute exacerbations (37, 38). ”Smoldering” inflammation in the tumor microenvironment has tumor-promoting effects, including enhanced tumor-cell migration, invasion, metastasis, epithelial-mesenchymal transition, and angiogenesis (29, 78). In addition, chronic inflammation also induces immunosuppression associated with accumulation of myeloid-derived suppressor cells (MDSCs) and regulatory T cells (Tregs), and related cytokine mediators (e.g., IL10 and TGFβ) (30, 31). However, the effects of bacterial-related chronic inflammation on lung tumorigenesis remain unclear.

Local immune responses and systematic inflammation are likely to influence the progression of tumors, which could alter treatment efficacy (40). Immunotherapy, such as checkpoint inhibitors, has emerged as a new treatment modality in lung cancer, yielding durable clinical responses (41, 42). However, the overall treatment response rate for non-small cell lung cancer (NSCLC) is around 15-20%, and only a minority of patients benefit from the treatment, possibly due to a lack of clear biomarkers or indications for the responders versus non-responders (24). Survival increases in PD-1 blockade recipients among NSCLC patients with COPD, suggesting that COPD-related dysregulated inflammation affects efficacy (43, 44). However, the mechanism of the effective immunotherapy remains unknown, and biomarkers used in the clinics

only partially predicted responding rates. This leaves a significant gap between the current diagnosis and the prognoses for lung cancer patients under immunotherapy (45).

The immune gene signatures recently identified include the transcripts encoding for cell surface markers, cytokines, cell signaling molecules, and transcription factors, which are indicative of specific immune-related responses (46). Immune-related gene signatures correlated with clinical responses in a subset of patients with solid tumors treated with checkpoint inhibitors (47, 49-51). However, the complete immune gene signatures in the animal models of lung cancer and in lung cancer patients associated with enhanced therapeutic and survival benefits have not been clearly identified.

To investigate the impact of chronic inflammation on lung tumorigenesis, we developed a two-staged lung cancer mouse model, which mimics the smoking carcinogen-induced, and COPD-related airway inflammation-promoted lung cancers in patients. We used the cigarette smoke carcinogen 4-(methylnitrosamino)-1-(3-pyridyl)-1-butanone (NNK) to generate genetic instability and parallelly provided repeated LPS to induce chronic lung inflammation. This exposure paradigm creates an immunosuppressive microenvironment favorable of tumor progression similar to that of inflammation-associated lung tumorigenesis. The model was used to evaluate the efficacy of anti-PD-1 immunotherapy. Our study provided a clinical-relevant lung cancer animal model in elucidating the effects of chronic inflammation on lung tumorigenesis and the efficacy of therapies.

3.2 Results

3.2.1 LPS-mediated chronic inflammation synergistically promotes NNK-induced lung tumorigenesis in mice

To explore the effect of LPS-mediated chronic inflammation on NNK-induced lung tumorigenesis, we established a murine lung cancer model by combining NNK exposure with recurring intranasal instillation of LPS during and after NNK administration (Figure 1A). Mice treated with NNK alone induced the average of 1.5 lung tumors per mice, while mice exposed to LPS alone generally did not have lung tumors except one tumor identified in all LPS-exposed mice (Figures 1B-C). However, combined exposure to NNK and LPS synergistically increased tumor numbers than NNK or LPS exposure alone (Figures 1B-C). Consistent with tumor multiplicity result was that 75 percent of mice developed lung tumors in NNK exposure, but 100 percent of mice developed lung tumors in the combined NNK plus LPS exposure (Figure 1D). In addition, tumor grade (alveolar hyperplasia, adenoma, and adenocarcinoma) and tumor area significantly increased in the combined exposure mice group than in the NNK-treated group (Figures 1E-F). Notably, NNK-induced lung tumors showed few inflammatory cells infiltrates (Figure 1G, panel 1 and 2), but tumors in combined exposure mice displayed an enhanced and distinct inflammatory cell infiltration phenotype, which recruited leukocytes infiltrating to the lung tumors (Figure 1G, panel 3 and 4, arrow).

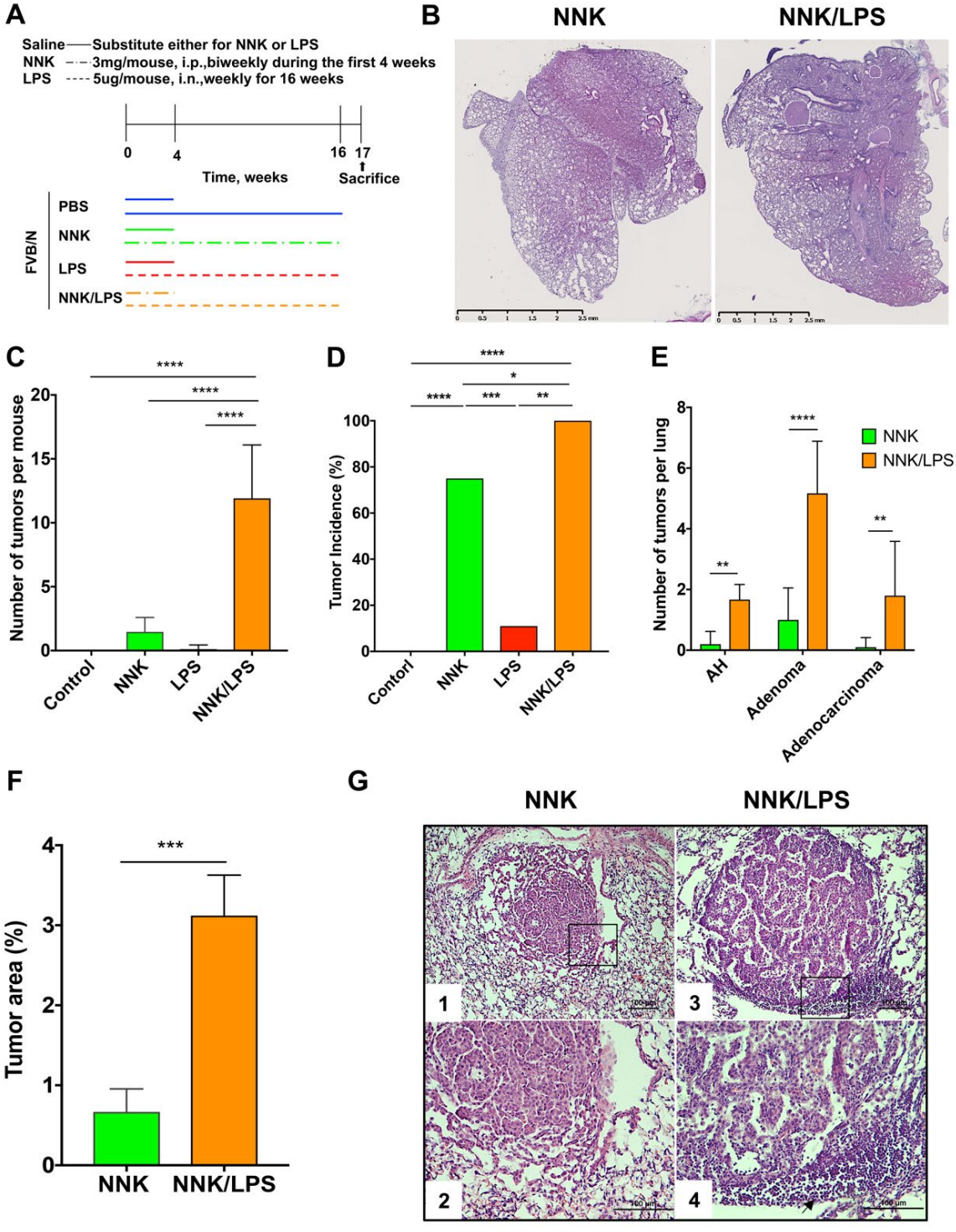
A
Saline——Substitute either for NNK or LPS
NNK - - -3mg/mouse, i.p.,biweekly during the first 4 weeks
LPS ----5ug/mouse, i.n.,weekly for 16 weeks
0
4
16
17
Sacrifice
Time, weeks
FVB/N
PBS
NNK
LPS
NNK/LPS
B
NNK
NNK/LPS
C
Number of tumors per mouse
Control
NNK
LPS
NNK/LPS
D
Tumor Incidence (%)
Contorl
NNK
LPS
NNK/LPS
E
Number of tumors per lung
NNK
NNK/LPS
AH
Adenoma
Adenocarcinoma
F
Tumor area (%)
NNK
NNK/LPS
G
NNK
NNK/LPS
1
2
3
4

Figure 1. Chronic exposure to LPS promotes NNK-induced lung tumorigenesis.

(A) Seven-week-old female FVB/NJ mice were exposed with NNK (3mg/mouse, intraperitoneal injection semi-weekly for first 4 weeks), LPS (5μg/mouse, weekly intranasal instillation for 16 weeks), or combined NNK and LPS. (B) H&E staining of tumor-bearing lungs. (C) Quantification of tumor number in mice exposed to PBS control (n=5), LPS (n=9), NNK (n=15) or NNK/LPS (n=11), Data shown are mean ± S.D., ****P < 0.0001 using one-way ANOVA. (D) Tumor incidence rate (%) in various exposure group was calculated, *P < 0.05, **P < 0.01, ***P < 0.001, ****P < 0.0001 using Chi-squared test. (E) The number of alveolar hyperplasia, adenoma and adenocarcinoma in NNK compared to NNK/LPS exposure as quantified, Data shown are mean ± S.D., **P < 0.01, ****P < 0.0001 using two-way ANOVA. (F) Tumor area (%) was calculated in NNK (n=4) and NNK/LPS exposure (n=4), Data shown are mean ± S.D., ***P < 0.001 using Student's t- test. (G) H&E staining of tumors derived from NNK and NNK/LPS-treated mice. Bottom, high-magnification images. The arrow defines tumor-infiltrating leukocytes. Scale bars, 100 μm. AH = alveolar hyperplasia; i.n. = intranasal; i.p. = intraperitoneal; PBS = Phosphate-buffered saline.

3.2.2 Chronic exposure to LPS increases inflammatory cells and alters cytokines/chemokines in the lung

To investigate the impact of LPS-mediated chronic inflammation in the lung, we analyzed the total cellular and cytokines/chemokines profiles in the BALF and lung protein extracts. The results showed that there was no significant difference in total and differential inflammatory cell count in BALF between control and NNK-treated mice (Figures 2A-B). Nevertheless, the total numbers of inflammatory cell in BALF increased and various inflammatory cells including macrophages, neutrophils, and lymphocytes all significantly increased in the presence of chronic LPS exposure regardless NNK treatment (Figures 2A-B). Consistent with the result was that the cytokines/chemokines analysis showed minor changes between control and NNK exposure, but increased IFN-γ, IP-10, IL-17, G-CSF, KC, MIP-1α levels in the presence of LPS exposure, especially in the NNK and LPS combined exposure (Figures 2C-H). Notably, combined exposure

to NNK and LPS synergistically increased G-CSF levels, which has been reported to correlate with granulocytic MDSC recruitment and development (Figure 2F) (79).

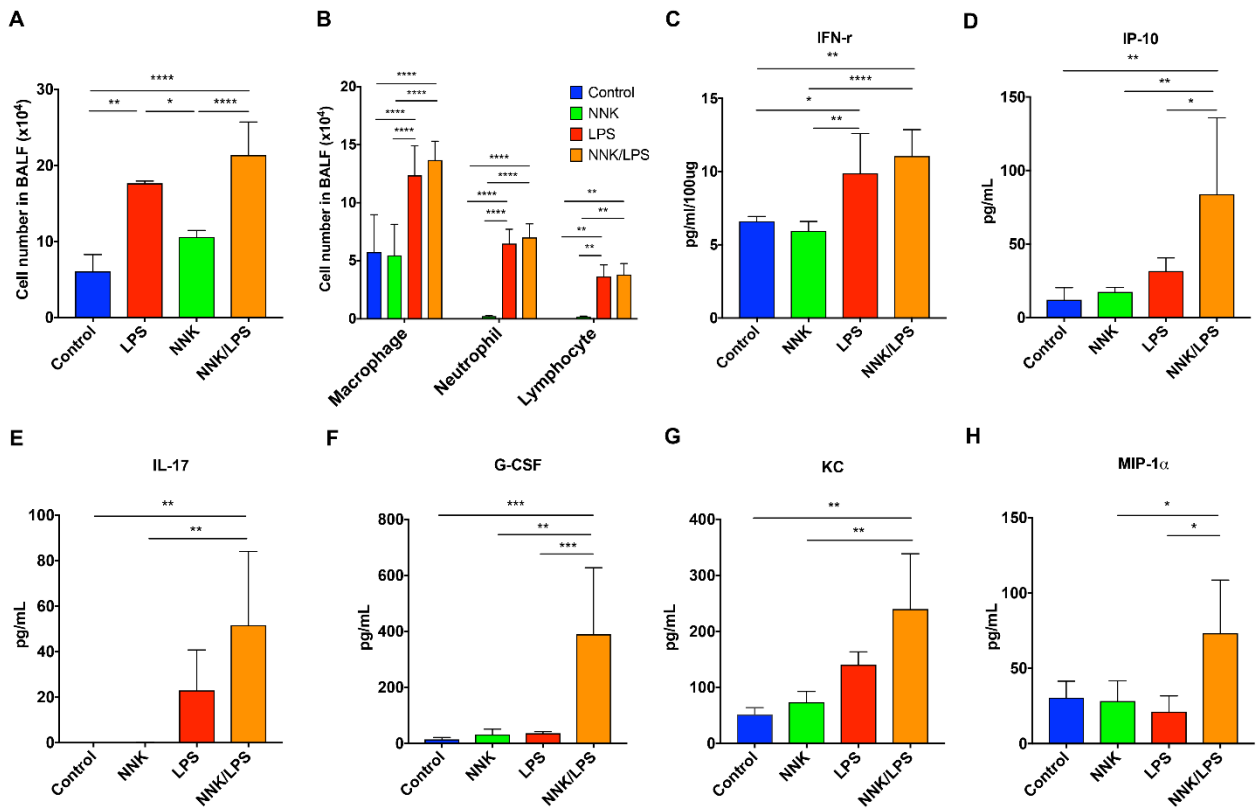

Figure 2. Chronic exposure to LPS increases lung inflammatory cells and alters cytokines and chemokines profile.

(A) Quantification of total cell number from bronchoalveolar lavage of different exposure groups (n=5 for each individual group). (B) Differential cell counts of inflammatory cells in BAL. (C-H) Cytokines/Chemokines in BAL and protein extracts (n=5 for each individual group) from different exposure groups were analyzed by Luminex assay and enzyme-linked immunosorbent assay. Data were collected from the samples harvested 17 weeks after treatment as shown by Figure 1A, and presented as the mean ± S.D. *P < 0.05, **P < 0.01, ***P < 0.001, ****P < 0.0001 using one-way ANOVA.

3.2.3 Combined exposure to NNK and LPS increase the accumulation of immunosuppressive cells in the lung

To identify the profile of the increased immune cell population in the lungs of tumor-bearing mice, we performed the immune cell profiling of lung tissue by flow cytometry. NNK exposure alone showed higher number of CD4+ T helper cells such as Th1, Th17, and Tregs, MDSCs, and CD8 cytotoxic T cells (Tc1) compared to control, but there was no statistical difference (Figures 3A-F). LPS exposure alone increased Th17 cells compared to control and NNK exposure (Figure 3B). However, combined NNK and LPS exposure significantly increased Th1, Th17, Tregs, and MDSCs compared to other exposure groups (Figures 3A-F). Importantly, immunosuppressive cells such as MDSCs and Tregs in the combined exposure group were significantly increased in the mouse lungs, suggesting the immunosuppressive microenvironment. The slightly increased Tc1 after combined exposure did not reach a statistically significant difference compared to other exposure groups (Figure 3F).

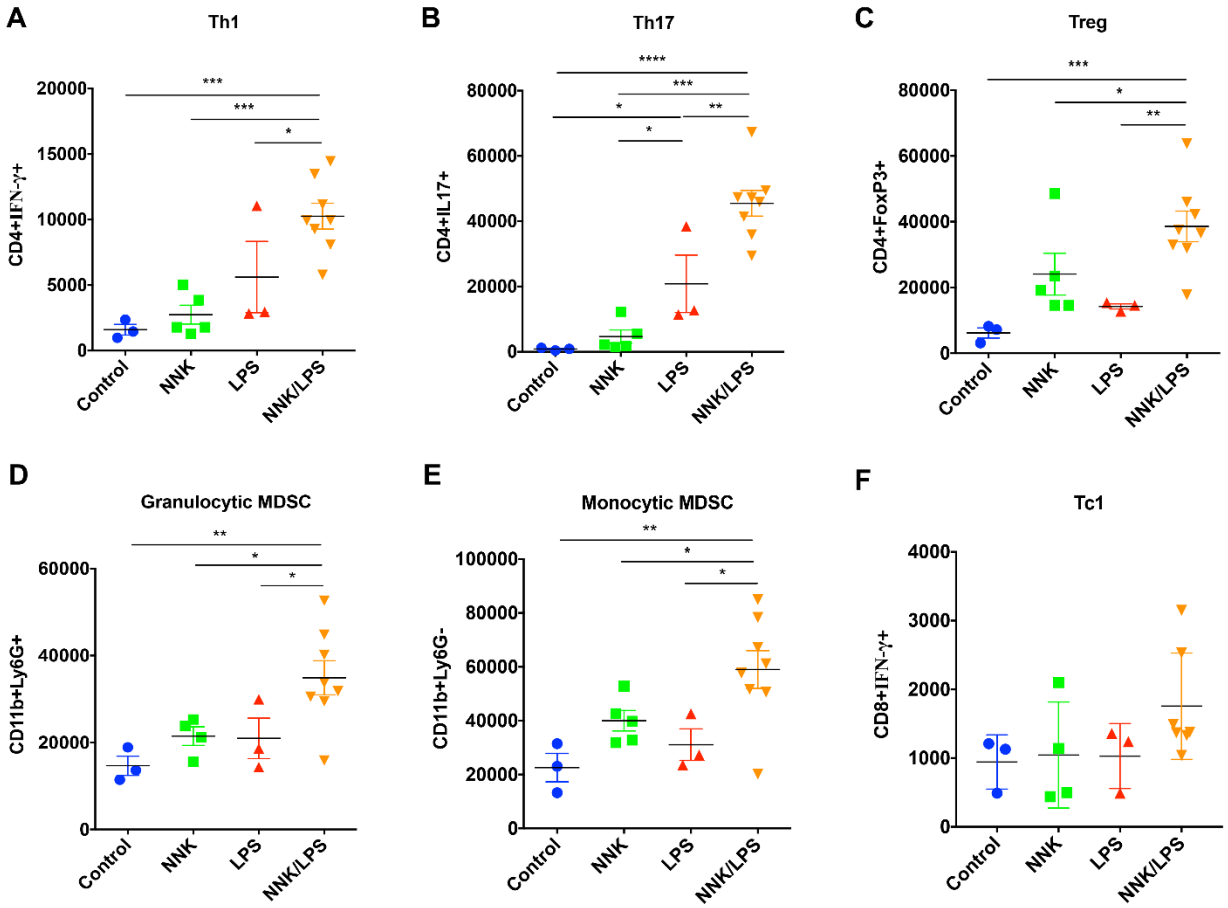

Figure 3. Combined exposure of NNK and LPS increases accumulation of immunosuppressive cells in the lungs.

Flow cytometry analysis of immune cell population of mouse lungs in different exposure groups harvested at week 17 after NNK and LPS treatment as indicated in Figure 1A. The cellular markers included (A) Th1, (B) Th17, (C) Tregs, (D) Granulocytic MDSCs, (E) Monocytic MDSCs, and (F) Tc1. Data shown are mean ± S.D. *$P < 0.05$, **$P < 0.01$, ***$P < 0.001$, ****$P < 0.0001$ using one-way ANOVA. Th1 = T-helper cell type 1; Th17 = T-helper cell type 17; Treg = regulatory T cell; MDSC = myeloid-derived suppressor cell; Tc1 = $CD8^+$ cytotoxic T lymphocyte.

3.2.4 Chronic exposure to LPS correlates with T-cell exhaustion and immune cell gene signatures

To elucidate the mechanisms of LPS-mediated inflammation in NNK-induced lung tumorigenesis, we performed the mRNA microarray analysis of mouse lung tissue from different exposure groups. Unsupervised hierarchical clustering heatmap revealed two sample groups clustered with the differentially expressed genes between NNK/LPS and NNK. The first one included control and NNK-treated groups, while the other one showed LPS and NNK/LPS-treated groups were clustered together (Figure 4A). A gene cluster showed that lymphocyte recruitment related chemokine genes such as *Cxcl9, Cxcl10, Cxcl13,* and *Ccl20* were increased expression in the presence of chronic exposure to LPS (Figure 4A). IPA based on the differentially expressed genes showed multiple pathways involved in T-cell immune responses with high statistical significance (Figure 4B). Since antigen overstimulation has been shown to correlate with T cell exhaustion (80), we hypothesized that chronic LPS exposure may result in T cell exhaustion. Therefore, we checked inhibitory receptors related genes by real-time PCR, and the results demonstrated that the expression of *Pdcd1, Ctla4, Lag3,* and *Tim3* were all increased after chronic LPS exposure (Figure 4C). Importantly, *Pdcd1* showed the highest expression with the 10-fold increase among these inhibitory receptor genes in combined NNK and LPS exposure compared to NNK exposure alone. In addition, we performed hierarchical clustering analysis of the mouse genes (Figure 4D), based on the immune gene signature identified from the NSCLC patient cohort under the immunotherapy presented later by Figure 6. Overall, immune cell gene signature expression such as T cell, B cell, and Th17 cell increased in the presence of chronic exposure to LPS compared to NNK and control groups (Figure 4E). However, NNK-treated mice showed

decreased NK cell signature regardless of LPS exposure compared to the control group, indicative of immunosuppression (Figure 4E).

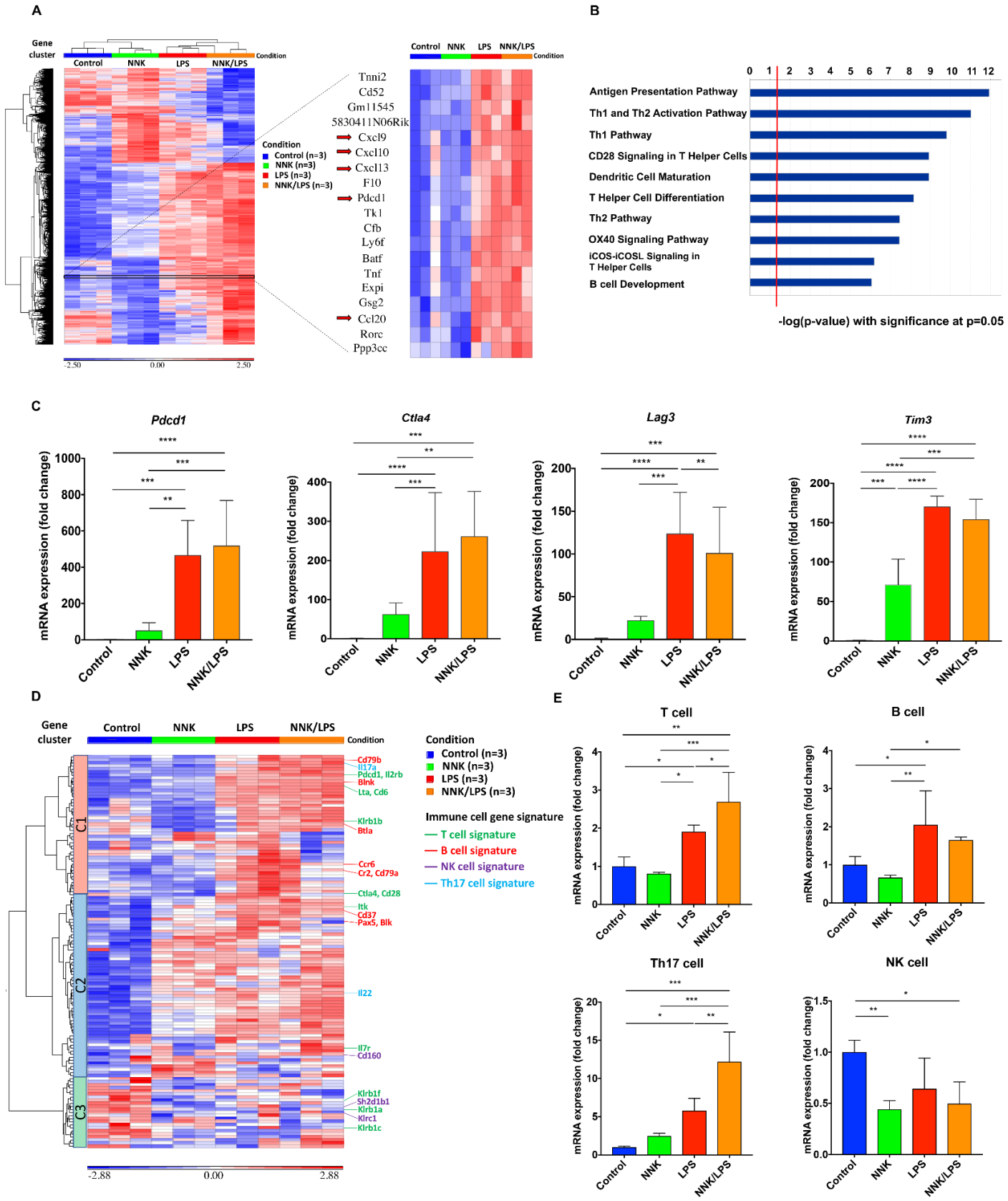
A
Gene cluster
Control
NNK
LPS
NNK/LPS
Condition
Control (n=3)
NNK (n=3)
LPS (n=3)
NNK/LPS (n=3)
-2.50
0.00
2.50
Tnni2
Cd52
Gm11545
5830411N06Rik
Cxcl9
Cxcl10
Cxcl13
F10
Pdcd1
Tk1
Cfb
Ly6f
Batf
Tnf
Expi
Gsg2
Ccl20
Rorc
Ppp3cc
B
Antigen Presentation Pathway
Th1 and Th2 Activation Pathway
Th1 Pathway
CD28 Signaling in T Helper Cells
Dendritic Cell Maturation
T Helper Cell Differentiation
Th2 Pathway
OX40 Signaling Pathway
iCOS-iCOSL Signaling in T Helper Cells
B cell Development
-log(p-value) with significance at p=0.05
C
Pdcd1
Ctla4
Lag3
Tim3
mRNA expression (fold change)
D
C1
C2
C3
Cd79b
Il17a
Pdcd1, Il2rb
Blnk
Lta, Cd6
Klrb1b
Btla
Ccr6
Cr2, Cd79a
Ctla4, Cd28
Itk
Cd37
Pax5, Blk
Il22
Il7r
Cd160
Klrb1f
Sh2d1b1
Klrb1a
Klrc1
Klrb1c
Immune cell gene signature
T cell signature
B cell signature
NK cell signature
Th17 cell signature
E
T cell
B cell
Th17 cell
NK cell

Figure 4. LPS-mediated chronic inflammation correlates with T-cell exhaustion and immune cell gene signatures.

The mRNA microarray data of mouse lung tissues (n=3 for each individual group) were analyzed. (A) Unsupervised hierarchical clustering heatmap based on the differentially expressed genes (n=1179, absolute fold change >2, false discovery rate <0.05) between NNK/LPS and NNK. Lymphocyte recruitment related genes such as *Cxcl9*, *Cxcl10*, *Cxcl13*, and *Ccl20* were labeled (arrows). (B) Ingenuity pathway analysis based on the differentially expressed genes showed significant pathways. (C) The inhibitory checkpoint receptors genes expression: *Pdcd1*, *Ctla4*, *Lag3*, and *Tim3* in various exposure groups were quantified by quantitative real-time polymerase chain reaction. (D) Hierarchical clustering heatmap based on mouse ortholog genes of immune gene panel (n=127) identified from GSE93157 cohort. (E). Immune cell gene signatures including T cell, B cell, NK cell, and Th17 cell were quantified in different exposure groups. Data shown are mean ± S.D. $^{**}P < 0.01$, $^{***}P < 0.001$, $^{****}P < 0.0001$ using one-way ANOVA.

3.2.5 Combined exposure to NNK and LPS upregulates PD-1/PD-L1 axis in the tumor microenvironment

Our results showed that combined exposure to NNK and LPS involved in T-cell mediated immunity pathways with increased inhibitory receptor genes expression, suggestive of T cell exhaustion. To characterize the tumor-infiltrating T lymphocytes and PD-1 expression in the tumor microenvironment, we performed multiplex immunohistochemical staining of CD4, CD8, and PD-1 in tumor-infiltrating T lymphocytes (Figure 5A). The results demonstrated that there were much less tumor-infiltrating T lymphocytes (CD4+ and CD8+) and PD-1-expressed cells in lung tumors of NNK-treated mice than in NNK/LPS-treated mice (Figure 5B). In addition, PD-1 colocalized with tumor-infiltrating CD4 and CD8 T lymphocytes, especially in NNK/LPS-treated lung tumors (Figure 5B). Western blot analysis showed increased PD-L1 expression in mouse lung-protein extracts from NNK/LPS-treated mice than those from NNK-treated mice (Figure 5C). Furthermore, the IHC staining results also confirmed increased PD-L1 expression that lung tumors from NNK/LPS-treated mice showed significantly increased positive PD-L1 staining than tumors from NNK-treated mice (Figure 5D).

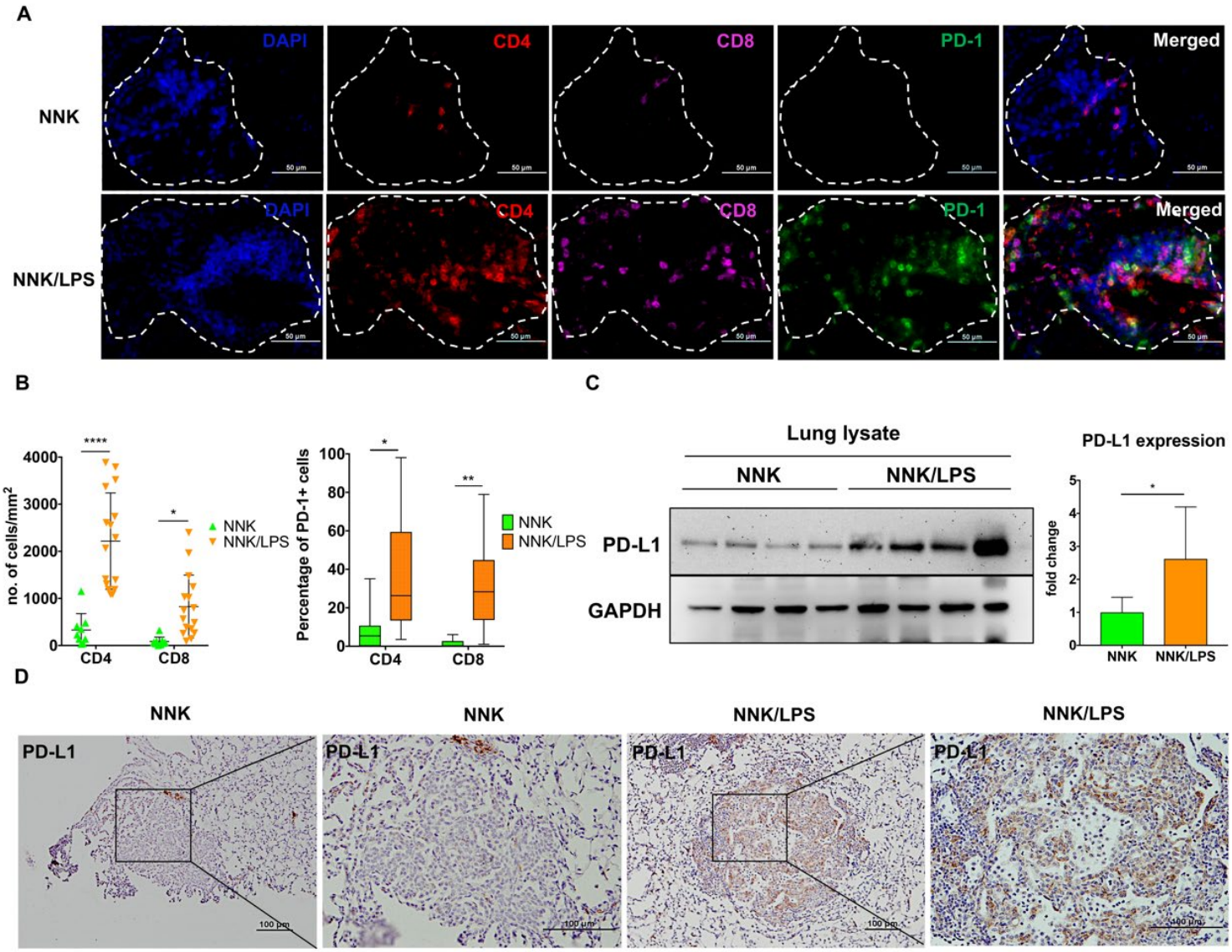

Figure 5. Combined NNK/LPS exposure increases TILs with co-localized PD-1 and upregulates tumor PD-L1 expression.

(A) Representative immunofluorescence images of CD4 (red), CD8 (Magenta), PD-1 (green), and nuclear staining with DAPI (blue) in tumor infiltrating cells. 400x magnification. Scale bars, 50 μm. Dotted lines outline tumors. (B) Quantification of $CD4^+$ and $CD8^+$ TILs. The percentage of PD-1 expression on $CD4^+$ and $CD8^+$ TILs was shown. *$P < 0.05$, **$P < 0.01$, ****$P < 0.0001$ using two-way ANOVA. (C) Lung lysates from NNK (n=4) and NNK/LPS-treated mice (n=5) were quantified for PD-L1 expression. *$P < 0.05$ using Student's *t*-test. (D) Representative images for PD-L1 IHC staining. Right, high-magnification images. Scale bars, 100 μm. DAPI = 4',6-Diamidino-2-Phenylindole, IHC = immunohistochemistry; PD-1 = programmed cell death 1; PD-L1 = programmed death-ligand 1; TIL = tumor infiltrating lymphocytes.

3.2.6 Elevated inflammatory responses correlate with PD-1 blockade efficacy

Based on the increased PD-1/PD-L1 pathway in NNK/LPS-treated mice, we examined if the PD-1/PD-L1 checkpoint pathway blockade could inhibit inflammation-associated lung tumorigenesis. We performed a separate pilot study and observed that the detection of the first lung tumor was frequently identified at 10-week after LPS installation in NNK-treated mice. Therefore, NNK-treated mice or plus 10-week LPS installation received either control IgG or anti-PD-1 antibody starting at 10-week after LPS installation for 6 consecutive weeks (Figure 6A). The anti-PD-1 treatment effectively decreased lung tumor numbers in NNK/LPS-treated mice, but the effect was not found in NNK-treated mice (Figure 6B). Consistent with the result of anti-PD-1 efficacy in decreasing tumor numbers, PD-1 blockade also decreased the tumor area in NNK/LPS-treated mice (Figure 6C). However, when we increased LPS installation for 16 weeks to NNK-treated mice, anti-PD-1 treatment only slightly decreased tumor number and tumor area compared to IgG control but did not reach a statistically significant difference (Figures 6E-F). Anti-Ly6G treatment to deplete MDSCs effectively decreased tumor number and tumor area compared to control IgG, indicating a dominant tumor-promoting effect of MDSCs (Figure 6E-F). Importantly, combined anti-PD-1 and anti-Ly6G significantly decreased tumor numbers and tumor area compared to anti-PD-1 or anti-Ly6G treatment alone, suggesting the enhanced anti-tumor activity by the combinatory treatment (Figures 6E-F).

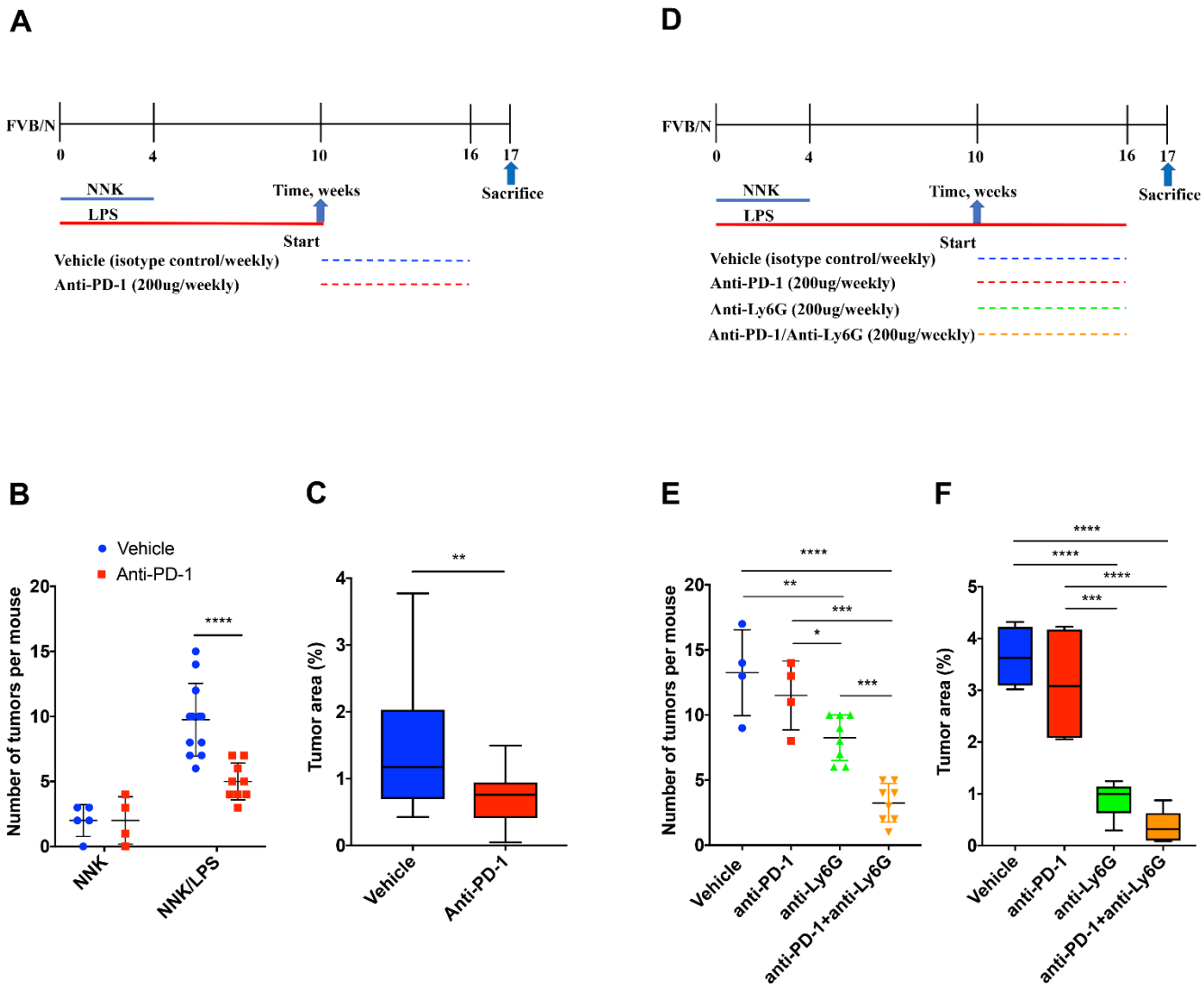

Figure 6. LPS-mediated inflammatory responses associated with PD-1 blockade efficacy.

(A) The treatment paradigm of anti-PD-1. Mice were exposed to NNK or NNK combined with 10-week LPS treated for either IgG control (IgG2a) or anti-PD-1 for 6 weeks. (B) Quantification of tumor numbers from mice in NNK and NNK/LPS groups with different treatment. ***$P < 0.001$ using Student's *t*-test. (C) Quantification of tumor area (%) in NNK/LPS-treated mice treated with IgG control (n=11) and anti-PD-1 (n=8). **P < 0.01 using Student's *t*-test. (D) The treatment paradigm of anti-PD-1 and anti-Ly6G. Mice were exposed to NNK or NNK combined with 16-week LPS treated for either IgG control (n=4), anti-PD-1 (n=4), anti-Ly6G (n=8) or combined anti-PD-1 and anti-Ly6G (n=8) for 6 weeks. (E) Quantification of tumor numbers harvested from each group. *$P < 0.05$, **$P < 0.01$, ***$P < 0.001$, ****$P < 0.0001$ using one-way ANOVA. (F) Quantification of tumor area (%) in NNK/LPS-treated mice treated with IgG control (n=4), anti-PD-1 (n=4), anti-Ly6G (n=5), anti-PD-1+anti-Ly6G (n=5). ***$P < 0.001$, ****$P < 0.0001$ using one-way ANOVA.

3.2.7 Immune gene signature correlates with PD-1 blockade responsiveness and progression-free survival in NSCLC patients

We analyzed transcriptomes from a cohort of 35 NSCLC patients involved in PD-1 blockade response (GSE93157; Table 1). We identified an immune gene panel, which contains 130 differentially expressed immune-related genes between nonprogressive disease (NPD) and progression disease (PD), and generated hierarchical clusters (Figure 7A). Overall, the transcriptomes of NPD patients displayed an increased immune-related gene expression compared to those of PD patients. Furthermore, we assessed the immune cell gene signatures for T-cells, B-cells, NK-cells, and Th17-cells. Most T-cell and B-cell associated markers localized to the C1 cluster, whereas NK-cell, Th17-cell, and other immune-related makers were observed in the other clusters (Figure 7A). Moreover, T-cell, B-cell, NK-cell, and Th17-cell signatures increased more in NPD than in PD patients, suggesting that the immunologically "hot" tumors could benefit from anti-PD-1 treatment. These immune cell gene signature results between patients with NPD and PD (Figure 7B) were similar to those between NNK/LPS- and NNK-treated mice (Figures 7D-E). In addition, the increased immune cell gene signature was also associated with prolonged progression-free survival (PFS) in patients with NSCLC treated with PD-1 blockade (Figure 7C). ROC analysis was performed to evaluate the diagnostic accuracy of these gene signatures to predict treatment responses (NPD versus PD) in GSE93157. The results showed that all signatures were with an area under curve > 0.7 and *P* value <0.05 (Figure 8).

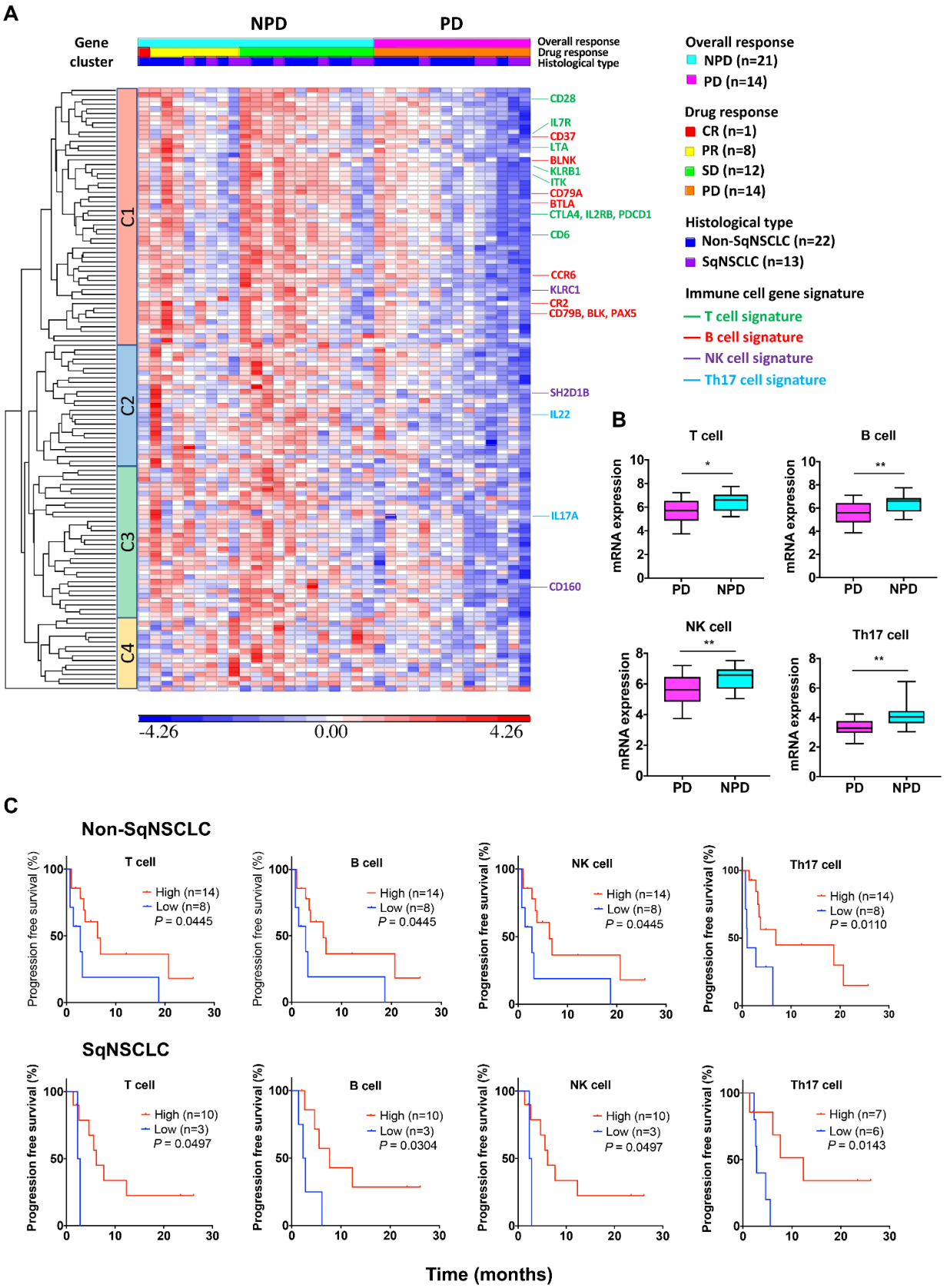
A
NPD
PD
Gene cluster
Overall response
Drug response
Histological type
C1
C2
C3
C4
CD28
IL7R
CD37
LTA
BLNK
KLRB1
ITK
CD79A
BTLA
CTLA4, IL2RB, PDCD1
CD6
CCR6
KLRC1
CR2
CD79B, BLK, PAX5
SH2D1B
IL22
IL17A
CD160
-4.26
0.00
4.26
Overall response
NPD (n=21)
PD (n=14)
Drug response
CR (n=1)
PR (n=8)
SD (n=12)
PD (n=14)
Histological type
Non-SqNSCLC (n=22)
SqNSCLC (n=13)
Immune cell gene signature
T cell signature
B cell signature
NK cell signature
Th17 cell signature
B
T cell
B cell
NK cell
Th17 cell
mRNA expression
PD
NPD
C
Non-SqNSCLC
SqNSCLC
Progression free survival (%)
High (n=14)
Low (n=8)
P = 0.0445
P = 0.0110
High (n=10)
Low (n=3)
P = 0.0497
P = 0.0304
High (n=7)
Low (n=6)
P = 0.0143
Time (months)

Figure 7. Immune gene signatures correlate with responses to PD-1 blockade and progression-free survival.

Tumor samples of 35 NSCLC patients before anti-PD-1 treatment were analyzed for the gene expression. (A) Expression profiles of 130 differentially expressed genes between NPD and PD were presented by heatmap where red indicates relative gene overexpression and blue indicates relative gene underexpression compared to means for each gene. Overall response (NPD; PD), drug response (CR; PR; SD; PD), and histological type (Non-SqNSCLC; SqNSCLC) are indicated at the top of the heatmap. Immune cell gene signatures including T cell, B cell, NK cell, and Th17 cell are labeled (B) Box plots for expression of gene signatures across patients that showed PD and NPD. $*P < 0.05$, $**P < 0.001$ using Student's *t*-test. (C) Kaplan–Meier survival analysis based on selected gene signatures in Non-SqNSCLC and SqNSCLC. *P* value was based on the log-rank test. CR = complete response; NK cell = natural killer cells; Non-SqNSCLC = non-squamous cell non-small cell lung cancer; NPD = non-progressive disease, including CR, PR, and SD; PD = progression disease; PR = partial response; SD = stable disease; SqNSCLC = squamous cell non-small cell lung cancer; Th17 = T-helper cell type 17.

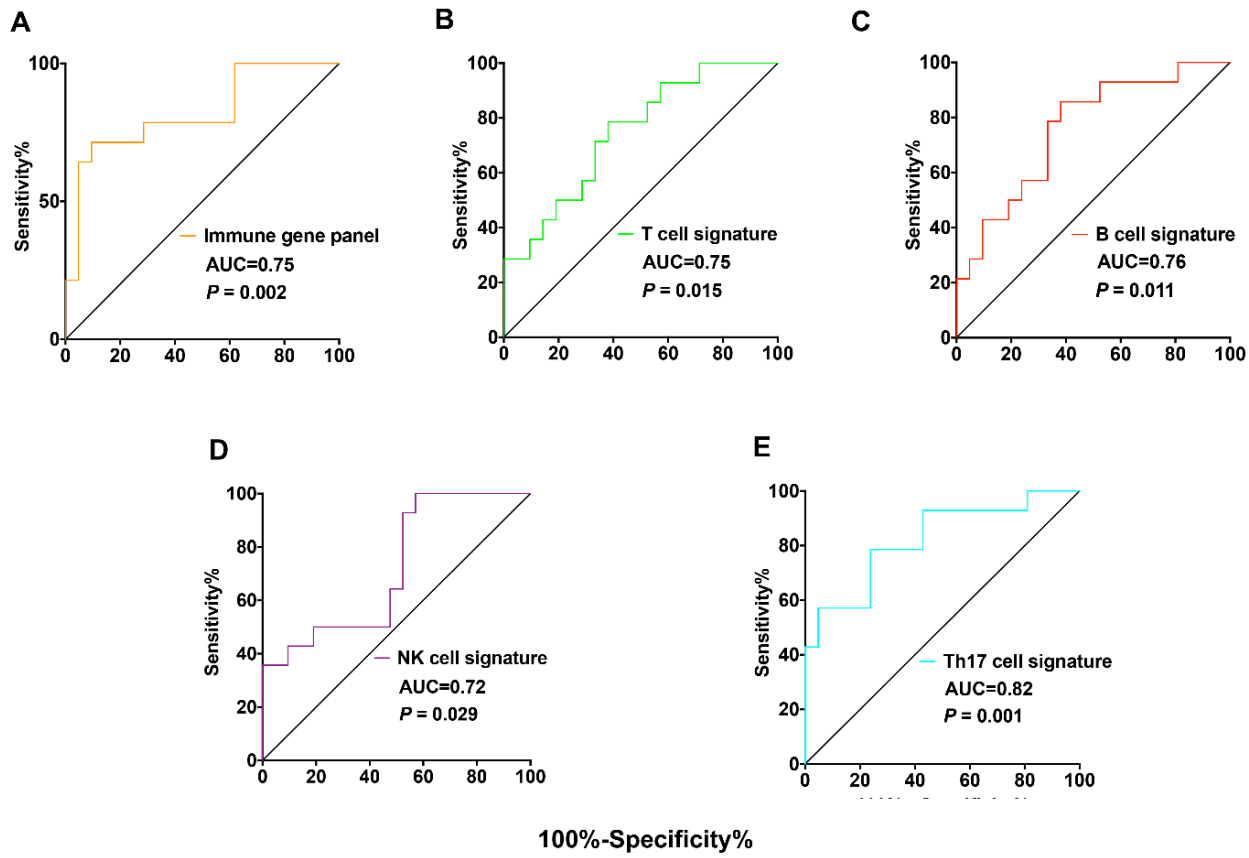

Figure 8. ROC analysis of immune gene signatures in GSE93157 cohort.

ROC analysis was performed on immune gene panel and individual immune cell gene signatures in GSE93157 cohort of 35 NSCLC patients. The Area under the curve of (A) immune gene panel, (B) T-cell signature, (C) B-cell signature, (D) NK-cell signature, (E) Th17-cell signature was calculated. Statistical significance is attained when $p < 0.05$.

Table 1. Clinical Characteristics of NSCLC patients with anti-PD-1 treatment from GSE93157 cohort.

Characteristics	*N* (%)
Subject, *n*	35
Sex, M/F, *n* (%)	27/8 (77/23)
Age, yr, mean ± SD	59 ± 11
Histological type, *n* (%)	
Nonsquamous lung carcinoma	22 (63%)
Squamous lung carcinoma	13 (37%)
Drug response, *n* (%)	
CR	1 (3%)
PR	8 (23%)
SD	12 (34%)
PD	14 (40%)
Overall response, *n* (%)	
Nonprogressive disease (CR, PR, SD)	21 (60%)
Progression disease (PD)	14 (40%)
Smoking status, *n* (%)	
Current smoker	10 (29%)
Former smoker	22 (63%)
Never smoker	3 (8%)
ECOG, *n* (%)	
0	11 (31%)
1	24 (69%)
Drug, *n* (%)	
Nivolumab	18 (51%)
Pembrolizumab	17 (49%)
PFS, median (95% CI)	3.2 (3.94−8.90)
EGFR status, *n* (%)	
EGFR mutated	1 (3%)*
EGFR wild-type	30 (86%)
NA	4 (11%)
ALK status, *n* (%)	
ALK rearranged	0 (0%)
ALK not rearranged	30 (75%)
NA	5 (25%)

Clinical–pathologic characteristics of patients with advanced NSCLC (n=35) and anti-PD-1 treatment from GSE93157 cohort were evaluated in this study. *Patients previously treated with EGFR tyrosine kinase inhibitor. *Definition of abbreviations:* ALK = Anaplastic lymphoma kinase; CI = confidence interval; CR = complete response; ECOG = Eastern Cooperative Oncology Group; EGFR = epidermal growth factor receptor; NSCLC = non-small cell lung cancer; SD = stable disease; PD = progression disease; PFS = progression-free survival; PR = partial response; NA = not applicable.

3.2.8 Immune gene signatures predict treatment responses and survival outcome in TCGA lung adenocarcinoma cohort

We sought to determine whether the immune gene signature could also predict treatment responses and survival outcome in patients with NSCLC under conventional treatment. We analyzed RNAseq of 517 TCGA lung adenocarcinomas (Table 2) using the immune gene panel (n=117), with the exclusion of 13 low expression genes. Overall, unsupervised hierarchical clustering revealed four subgroups of lung adenocarcinoma and the immune gene panel expression progressively decreased from subgroup 1 to 4. Remarkably, the immune cell gene signatures of T- and B-cell were in cluster 1, a similar pattern observed in GSE93157 cohort (Figure 9A). Patients with higher immune gene panel expression had better treatment responses and overall survival than those with lower expression (Figures 9B-C). Patients with increased immune gene panel expression had better treatment responses and overall survival than those with lower levels (Figures 9B-C and Figure 10A). We also analyzed the clinical characteristics in these groups and the results revealed that stage, mutation status, primary treatment response, and smoking status were differentially distributed between groups (Figure 9D and Figure 10B). In the subset of immune cell gene signature analysis, we performed unsupervised hierarchical clustering of lung adenocarcinomas based on immune cell gene signatures of T-cell, B-cell, and NK-cell (Figure 11A, Figure 12A, and Figure 13A). Consistently, patients with high immune cell gene signatures of T-cell, B-cell, and Th17-cell showed better survival outcome (Figure 11B, Figure 12B, and Figure 13B). Importantly, the patient cluster with increased immune gene panel expression remains an independent protective factor for overall survival in lung adenocarcinoma patients after adjustment of stage, gender, age, smoking, and mutation status (Table 3).

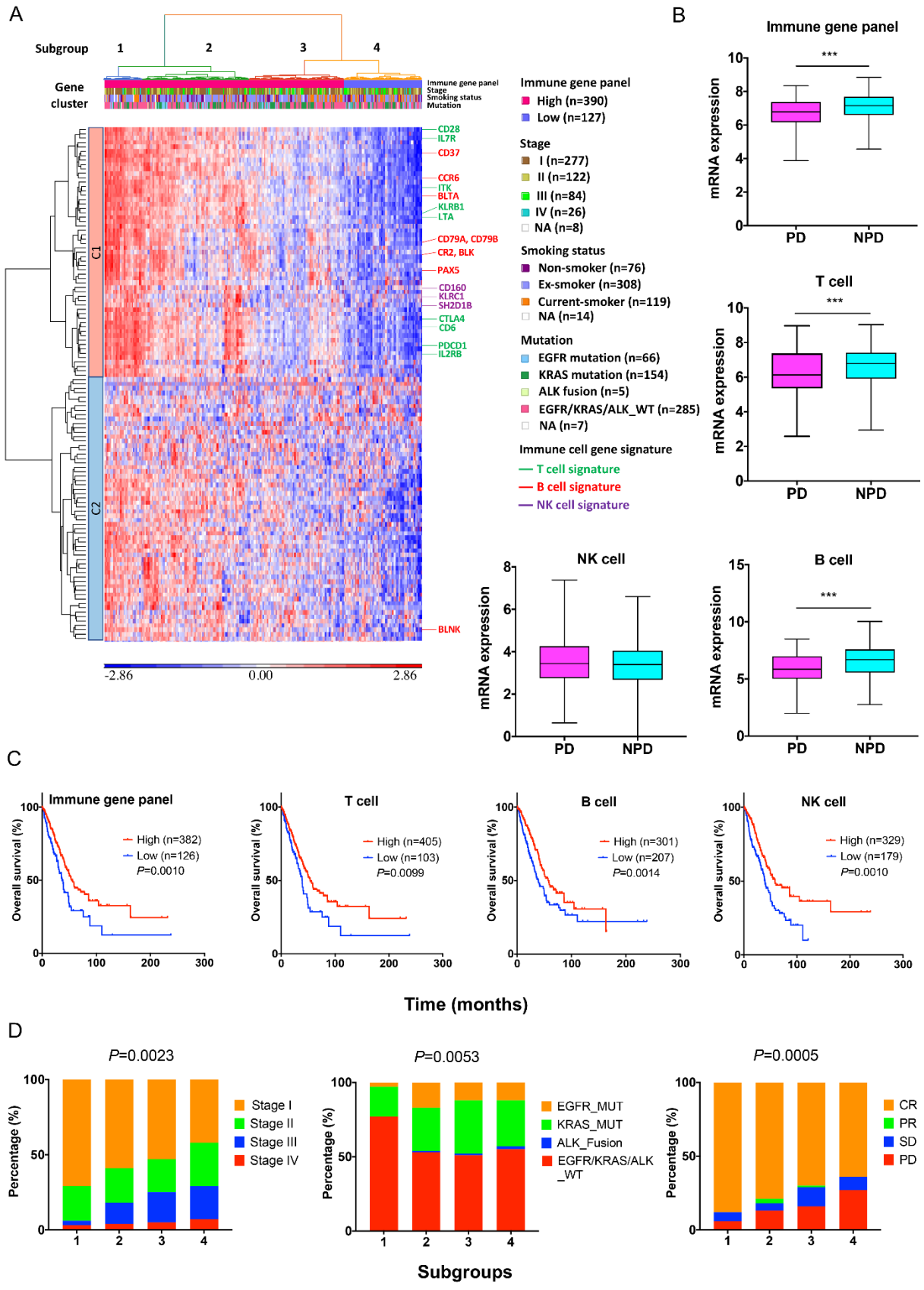
A
Subgroup
1
2
3
4
Gene cluster
Immune gene panel
Stage
Smoking status
Mutation
C1
C2
CD28
IL7R
CD37
CCR6
ITK
BLTA
KLRB1
LTA
CD79A, CD79B
CR2, BLK
PAX5
CD160
KLRC1
SH2D1B
CTLA4
CD6
PDCD1
IL2RB
BLNK
-2.86
0.00
2.86
Immune gene panel
High (n=390)
Low (n=127)
Stage
I (n=277)
II (n=122)
III (n=84)
IV (n=26)
NA (n=8)
Smoking status
Non-smoker (n=76)
Ex-smoker (n=308)
Current-smoker (n=119)
NA (n=14)
Mutation
EGFR mutation (n=66)
KRAS mutation (n=154)
ALK fusion (n=5)
EGFR/KRAS/ALK_WT (n=285)
NA (n=7)
Immune cell gene signature
T cell signature
B cell signature
NK cell signature
B
Immune gene panel
T cell
NK cell
B cell
mRNA expression
PD
NPD
***
C
Immune gene panel
High (n=382)
Low (n=126)
P=0.0010
T cell
High (n=405)
Low (n=103)
P=0.0099
B cell
High (n=301)
Low (n=207)
P=0.0014
NK cell
High (n=329)
Low (n=179)
P=0.0010
Overall survival (%)
Time (months)
D
P=0.0023
P=0.0053
P=0.0005
Percentage (%)
Stage I
Stage II
Stage III
Stage IV
EGFR_MUT
KRAS_MUT
ALK_Fusion
EGFR/KRAS/ALK_WT
CR
PR
SD
PD
Subgroups

Figure 9. Immune gene signatures correlate with treatment responses and survival outcome in TCGA lung adenocarcinoma cohort.

517 lung adenocarcinoma patient samples from the TCGA cohort were analyzed for the gene expression involved in immune gene signatures. (A) Expression profiles of immune gene panel (n=117) were identified from GSE93157 after filtered out the low expression genes. Immune-related genes are presented by heatmap where red indicates relative gene overexpression and blue indicates relative gene underexpression compared to means for each gene. Unsupervised hierarchical clustering revealed four lung adenocarcinoma subgroups clustered with immune gene panel. Immune gene panel, stage (I; II; III; IV), smoking status (non-smoker; ex-smoker; current smoker), mutation status (EGFR mutation; KRAS mutation; ALK fusion; EGFR/KRAS/ALK_WT) are indicated at the top of the heatmap. The T-cell, B-cell, and NK-cell gene signatures are color labeled. (B) Box plots show expression of gene signatures across patients with PD and NPD status. *$P < 0.05$, **$P < 0.001$ using Student's *t*-test. (C) Kaplan–Meier survival analysis of patient subgroups based on selected gene signatures using log-rank test. (D) Clinical characterization of four subgroups associated with immune gene panel as indicated in (A). The distribution difference among the four subgroups in the stage, mutation status, and primary treatment response was tested by Chi-squared test. ALK = Anaplastic lymphoma kinase; EGFR = epidermal growth factor receptor; KRAS = Kirsten rat sarcoma viral oncogene homolog; MUT = mutation; NA = not applicable; TCGA = The Cancer Genome Atlas; WT = wild type.

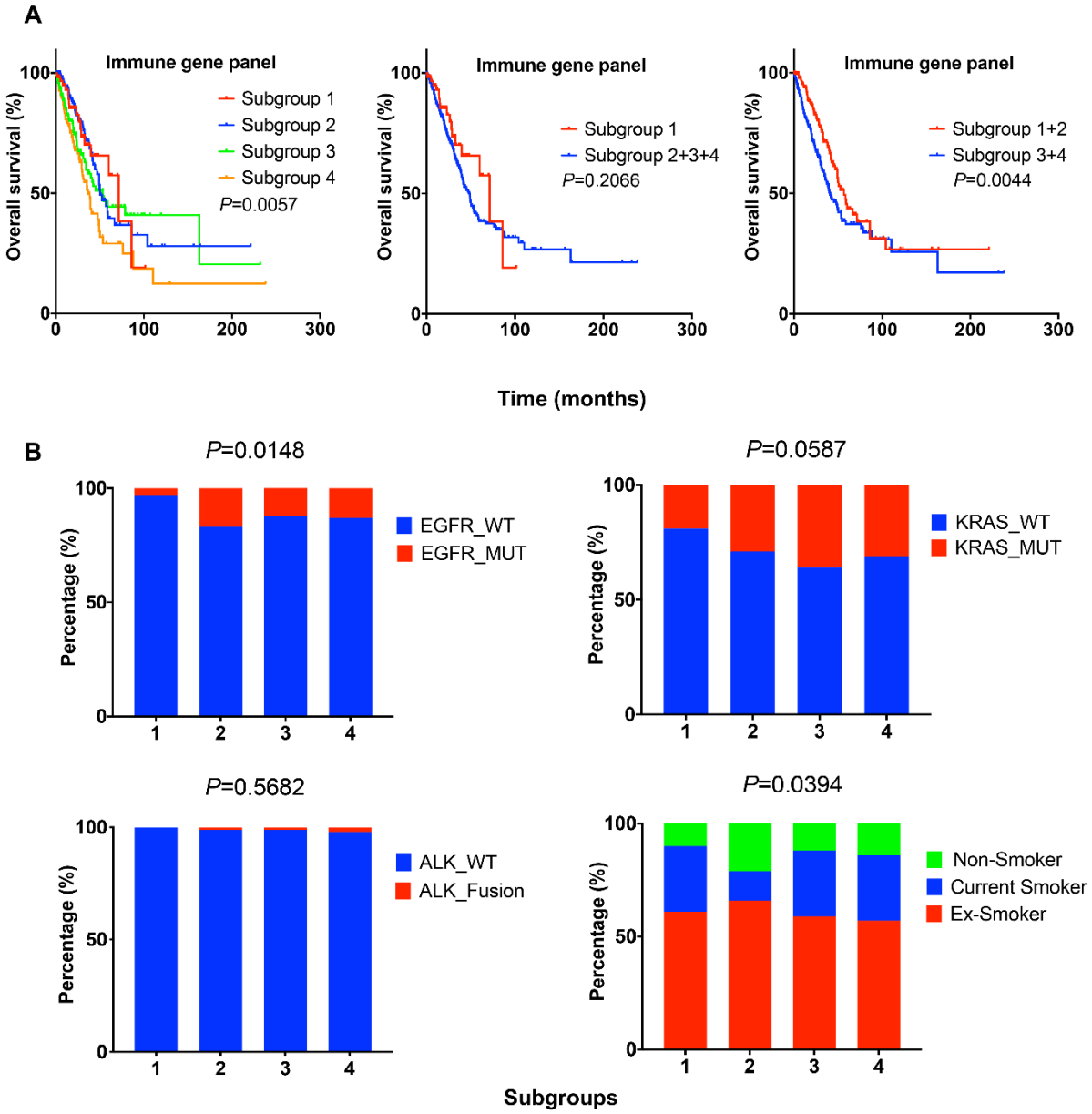

Figure 10. Immune gene panel expression correlates with overall survival and clinical characteristics in TCGA cohort.

Four subgroups of patients with lung adenocarcinoma determined by unsupervised hierarchical clustering with immune gene panel. (A) Kaplan–Meier survival analysis based on selected gene panel in different subgroups. *P* value was based on the log-rank test. (B) The distribution difference among the four subgroups in mutation subtype and smoking status was tested based on the Chi-squared test.

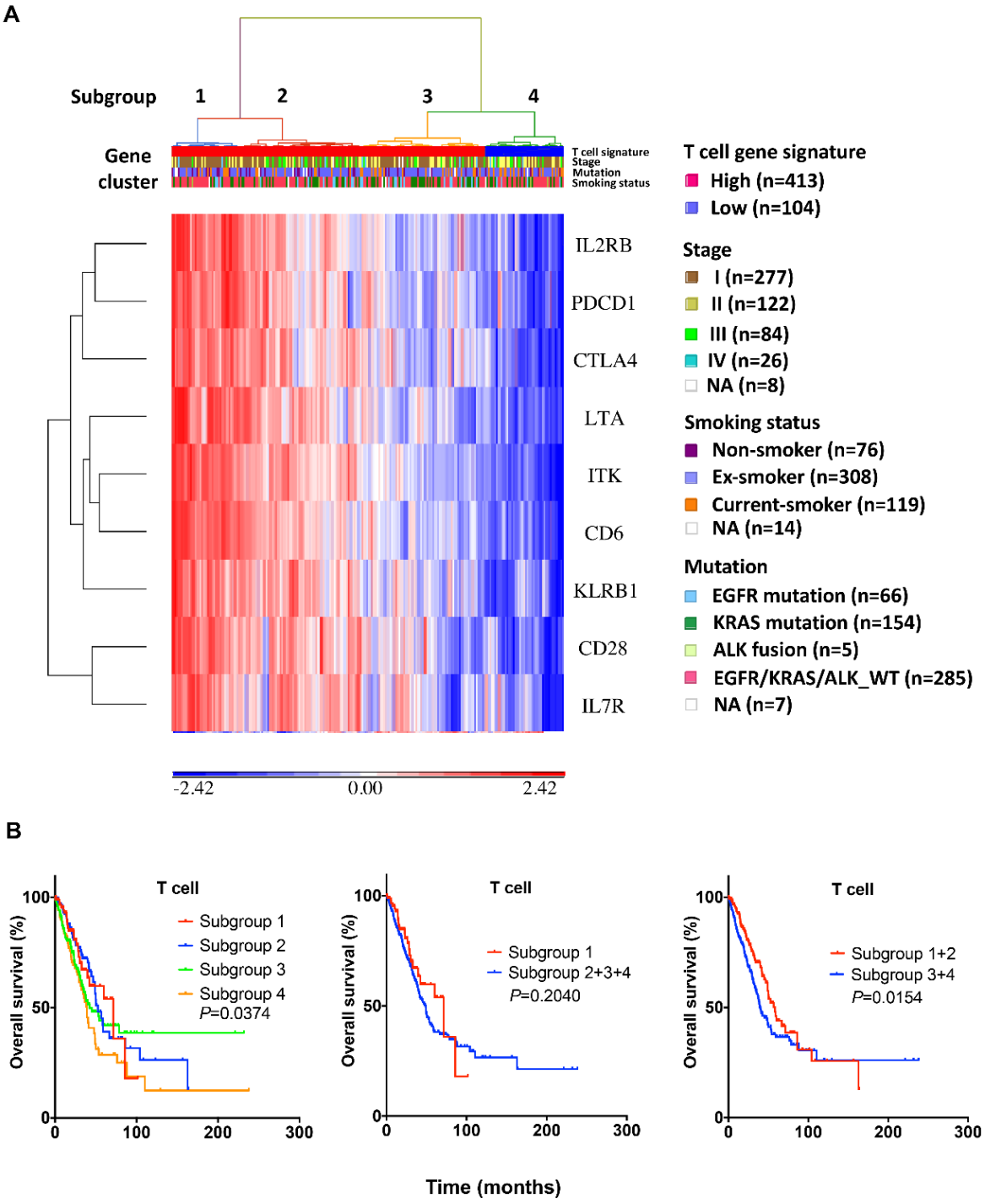

Figure 11. T-cell gene signature expression associated with overall survival in TCGA cohort.

(A) Expression profiles of T-cell gene signature are presented by heatmap. Four subgroups of patients with lung adenocarcinoma determined by unsupervised hierarchical clustering with T-cell gene signature. (B) Kaplan–Meier survival analysis based on selected gene signature in different subgroups. *P* value was based on the log-rank test.

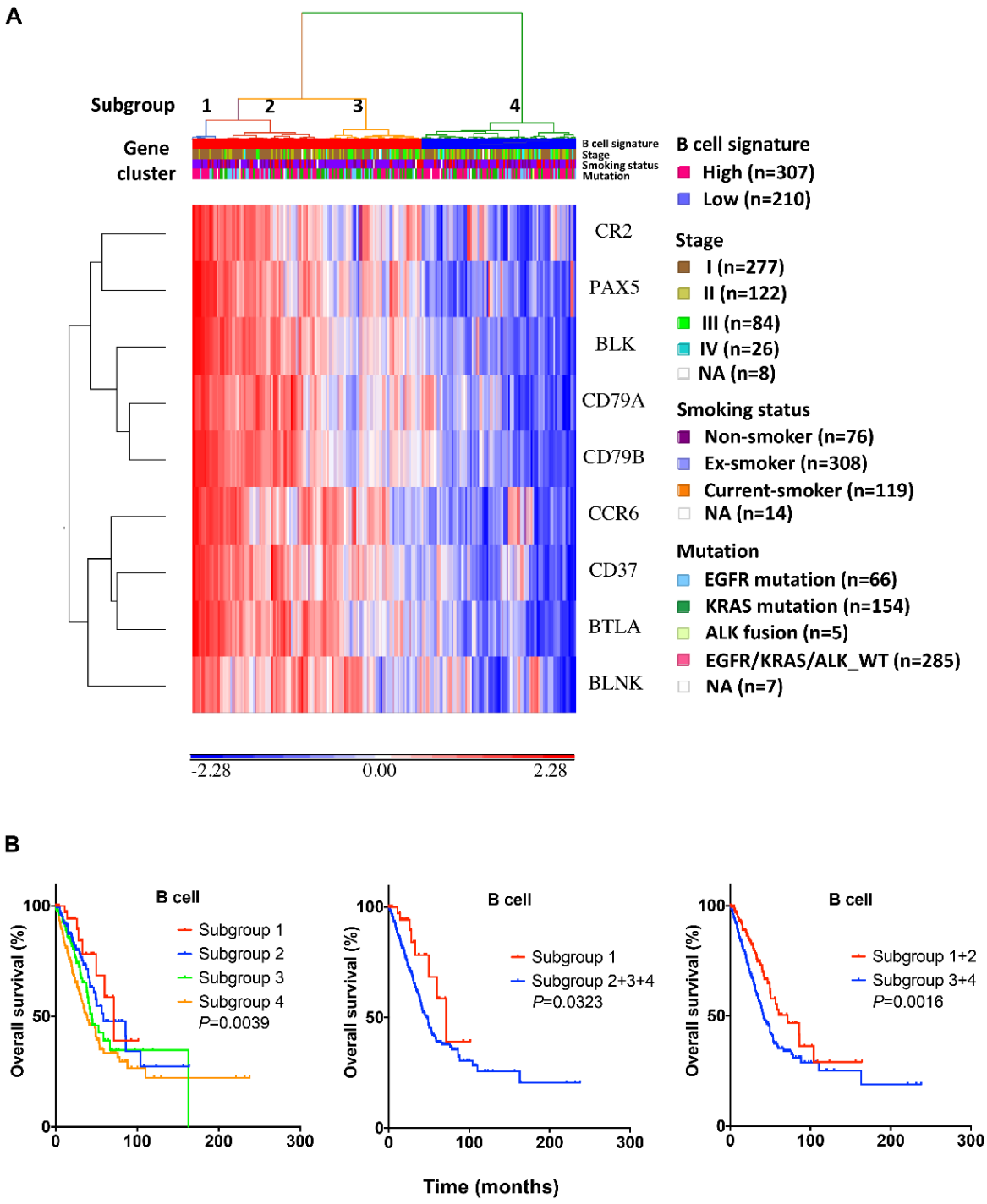

Figure 12. B-cell gene signature expression associated overall survival in TCGA cohort.

(A) Expression profiles of B-cell gene signature are presented by heatmap. Four subgroups of patients with lung adenocarcinoma determined by unsupervised hierarchical clustering with B-cell gene signature. (B) Kaplan–Meier survival analysis based on selected gene signature in different subgroups. *P* value was based on the log-rank test.

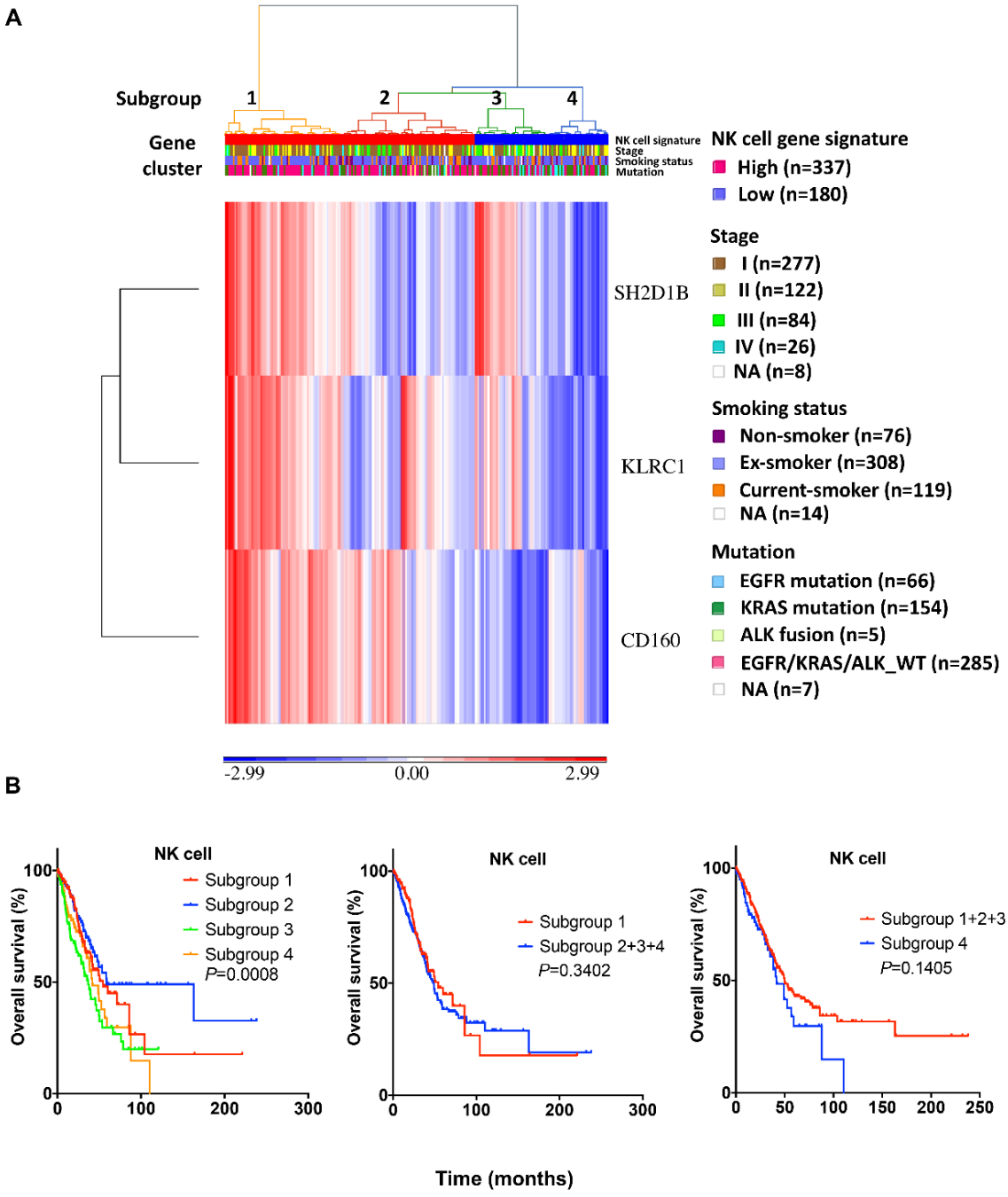

Figure 13. NK-cell gene signature expression associated with overall survival in TCGA cohort.

(A) Expression profiles of NK-cell gene signature are presented by heatmap. Four subgroups of patients with lung adenocarcinoma determined by unsupervised hierarchical clustering with NK cell gene signature. (B) Kaplan–Meier survival analysis based on selected gene signature in different subgroups. *P* value was based on the log-rank test.
patients with lung adenocarcinoma determined by unsupervised

Table 2. Clinical Characteristics of TCGA Lung Adenocarcinoma Cohort.

Characteristics	*N* (%)
Subjects, *n*	517
Sex, M/F, *n* (%)	240/277 (46/54)
Age, yr, mean ± SD	65 ± 13
pTNM stages	
I	277 (54)
II	122 (24)
III	84 (16)
IV	26 (5)
NA	8 (1)
Smoking status	
Non-smoker	76 (15)
Ex-smoker	308 (60)
Current-smoker	119 (23)
NA	14 (2)
Mutation status	
EGFR_MUT	66 (13)
KRAS_MUT	154 (30)
ALK _Fusion	5 (1)
KRAS/EGFR/AKL_WT	285 (55)
NA	7 (1)
ECOG	
0	62 (12)
1	58 (11)
2	17 (3)
3	5 (1)
4	2 (1)
NA	373 (72)
Treatment	
Surgery	386 (75)
Radiotherapy	43 (8)
Chemotherapy	155 (30)
Targeted therapy	18 (3)
Primary therapy response	
CR	296 (57)
PR	6 (1)
SD	34 (7)
PD	65 (13)
NA	156 (22)

Clinical–pathologic characteristics of TCGA lung adenocarcinoma cohort (n=517) were evaluated in this study. *Definition of abbreviations:* ALK = Anaplastic lymphoma kinase; CR = complete response; ECOG = Eastern Cooperative Oncology Group; EGFR= epidermal growth factor receptor; MUT = mutation; NA = not applicable; PD = progression disease; PFS = progression-free survival; PR = partial response; SD = stable disease; pTNM stages = pathologic TNM stages of malignant tumors; TCGA = the cancer genome atlas; WT = wild type.

Table 3. Predictors of Overall Survival in TCGA Lung Adenocarcinoma Cohort.

Characteristics	HR (95%)	*P* Value
Univariate predictors of OS		
Sex, M	1.13 (0.83−1.53)	0.4332
Age, per 1yr*	1.00 (0.99−1.02)	0.3618
pTMN stages		
II vs. I	2.27 (1.55−3.32)	**0.0165**
III vs. I	3.25 (2.17−4.83)	**0.0007**
IV vs. I	3.53 (2.03−6.13)	**0.0193**
Smoking status		
Current smoker vs. Non-smoker	0.89 (0.54−1.47)	0.6582
Ex-smoker vs. Non-smoker	0.97 (0.62−1.50)	0.8837
Mutation status		
EGFR_MUT vs. KRAS/EGFR/AKL_WT	1.56 (1.00−2.42)	**0.0466**
KRAS_MUT vs. KRAS/EGFR/AKL_WT	1.23 (0.92−1.84)	0.1378
ALK _Fusion vs. KRAS/EGFR/AKL_WT	0.0039 (0−Inf)	0.9990
Immune gene panel		
High vs. Low	0.61 (0.45−0.85)	**0.0028**
Multivariate predictors of OS		
pTMN stage		
II vs. I	2.19 (1.47−3.25)	**0.0001**
III vs. I	3.19 (2.12−4.80)	**0.0009**
IV vs. I	3.32 (1.86−5.93)	**0.0327**
Immune gene panel: High	0.66 (0.47−0.91)	**0.0124**

All variables were evaluated among the 470 patients with lung adenocarcinoma (47 patients excluded from 517 patients due to missing data).
Factors associated with OS in univariate and multivariate Cox regression model (n=470 patients). The HR (95%CI) and *P* value are shown for each. *P* value <0.05 are set in bold for emphasis.
*Additional risk with each additional year of age.
Definition of abbreviations: ALK = Anaplastic lymphoma kinase; EGFR = epidermal growth factor receptor; Inf = Infinite; KRAS = Kirsten rat sarcoma 2 viral oncogene homolog; MUT = mutation; OS = overall survival; TCGA = The Cancer Genome Atlas; WT= wild type.

3.3 Discussion

3.3.1 The characteristics of driver oncogene and immune contexture in the mouse model

Although several inflammation-associated lung cancer models have been proposed (81-83), these models are either genetically *Kras*-driven lung cancer or susceptible strain such as A/J mice, which showed 100% *Kras* mutation in chemically-induced lung tumors, which may not reflect human lung tumors heterogenicity (84). In addition, the effects of chronic inflammation on immune contexture contributing to lung tumorigenesis and its impacts on the efficacy of immune checkpoint inhibitors in these models have not been completely defined. Here, we used FVB/N mouse strain, which the activating mutation rates in *Kras* were 45.45% of NNK-treated lung tumors reported previously, which is close to the frequency of 32% *KRAS* mutations rate in human lung adenocarcinoma compared to other models (22, 63). In addition, we observed that LPS-mediated chronic inflammation increased various inflammatory cells including macrophages, neutrophils, and lymphocytes in the BALF, in agreement with other lung cancer models (81, 82). Notably in this model, significantly increased lung lymphocyte recruitment in the presence of chronic exposure to LPS, where T lymphocytes as the most affected population. Indeed, we observed significant pathways involved in T-cell mediated immunity and upregulated inhibitory receptor genes expression such as *Pdcd-1, Ctla4, Lag3,* and *Tim3* in NNK/LPS-treated mice than NNK-treated mice, which *Pdcd-1* showed the highest fold change increase. In agreement, our data showed that $CD4^+$ and $CD8^+$ TILs increased and colocalized with PD-1 in NNK/LPS-treated mice than NNK-treated mice, indicative of exhausted TILs. Interestingly, a recent study showed that patients with NSCLC and coexisting COPD increased exhausted $CD4^+$ and $CD8^+$ TILs with co-expression of PD-1, CTLA-4, LAG-3, and TIM-3, suggesting that chronic inflammation-mediated

dysregulated immune responses correlated with exhausted TILs, which shared common immune contexture with our model (43). Furthermore, we found that NNK/LPS-treated mice increased lung tumor PD-L1 expression compared to NNK-treated mice, which may correlate with the response to IFN-γ secretion by TILs and LPS-induced TLR-4 signaling (85, 86). Taken together, LPS-mediated chronic inflammation in NNK-treated mice increases TILs, inhibitory receptor genes expression, and upregulated PD-1/PD-L1 axis in the tumor microenvironment contributing to T cell exhaustion and diminishes antitumor immune surveillance.

3.3.2 The characteristics of immune gene signatures in the mouse model and lung cancer patients

In addition to the analysis of the phenotypic and functional characteristics of immune cells by flow cytometry, immunofluorescent staining and cytokine measurement in the mouse model, we performed transcriptome analysis using the published human immune gene signatures for human cancers. Here, we defined an overall immune gene signature and further stratified it into individual immune cell gene signatures, based on the presence in two or more studies of eight published signatures (46). These gene lists were transformed to the mouse homologues for the analysis of the mouse model, to reveal the similarity of the gene signatures between the mouse model and human lung cancer. In the mouse model, NNK/LPS-treated mice showed increased T cell gene signature expression indicative of T cell inflamed tumor microenvironment, which was associated with favorable efficacy of PD-1 blockade (87) consistent with the similar signature pattern in patients with NPD treated with PD-1 blockade (87). Interestingly, most T cell and B cell signature genes were clustered together in both mouse model and lung cancer cohorts with similar treatment responses and survival outcome, suggesting the potential antitumor immunity of B cell

and the possible B cell-T cell interaction of antigen presentation or antibody-mediated activities in the tumor microenvironment (70). In addition, mice treated with NNK regardless of LPS exposure decreased NK cell signature compared to control mice, indicating that cigarette carcinogen alone may mediate immunosuppression in the microenvironment. Although IL17 was reported to promote lung tumor progression through neutrophil infiltrate and mediate resistance to PD-1 blockade (88), we identified the higher Th17 cell signature expression associated with better anti-PD-1 response. This may reflect the complexity of immunologically "hot" tumors with various immune cell infiltration including immunosuppressive cells compared to "cold" tumors. Additionally, we explored the TCGA lung adenocarcinoma cohort using the same immune gene signatures. Consistently, patients with higher immune gene signature expression correlated with favorable treatment responses and overall survival than those with lower expression, regardless of treatment modality. These data support that these immune cell gene signatures are potential prognostic markers for the patient with NSCLC who received either immunotherapy or conventional treatments and provide a rationale for the combination therapeutics.

3.3.3 Inflammatory responses correlate immunotherapy efficacy

There is increasing evidence that the effectiveness of immunotherapy strategies relies on the presence of baseline immune responses and on unleashing of pre-existing immunity (89). In accordance with this hypothesis, NNK/LPS-treated mice showed favorable efficacy to PD-1 blockade compared to NNK-treated mice, suggesting that inflammation-associated lung cancer benefits from anti-PD-1 treatment. This is probably because LPS-induced chronic inflammation increased $CD4^+$ and $CD8^+$ TILs with PD-1 expression and upregulated tumor PD-L1 expression resulting in T cell exhaustion. Consequently, blockade of PD-1/PD-L1 axis abrogates tumor

growth through reversing exhausted T cells and restoring anti-tumor function in the tumor microenvironment. In this model of the tumor microenvironment, we also observed high percentages of myeloid cells that can be phenotypically divided into $CD11b^{+}Ly6G^{+}$ cells (Granulocytic MDSC, GrMDSC) and $CD11b^{+}Ly6G^{-}$ cells subsets, later include Monocytic MDSC (MoMDSC, $CD11b^{+}Ly6C^{+}$) and other myeloid cells (90). It has been reported that MDSCs in the tumor microenvironment may not only inhibit effector T cell and natural killer cell functions but also can directly promote tumor progression and metastasis (91). Our results showed that LPS-mediated chronic inflammation in NNK-treated mice synergistically increased G-CSF in BALF, which has been shown to involve GrMDSC development and recruitment (79). In addition, we observed that the IL17 also increased in NNK/LPS-treated mice, which has been reported to promote COPD-type inflammation promoted lung cancer progression through MDSCs infiltration (92, 93). In accordance with the result, NNK/LPS-treated mice with MDSC depletion significantly decreased tumor growth in the group with prolonged exposure of LPS. Furthermore, MDSCs in the tumor microenvironment are capable of converting naïve T cell to Tregs, contributing to immunosuppression (94). Taken together, the inflammatory cytokines/chemokines milieu induced by chronic exposure to LPS promotes MDSCs recruitment and tumor proliferation.

3.3.4 MDSCs depletion enhances immunotherapy efficacy

Immunosuppressed tumor microenvironment not only hinders natural host immune responses, but also the efficacy of cancer immunotherapies (89). We observed that prolonged exposure to LPS not only recruited TILs but also increased MDSCs and Tregs accumulation, which have been reported to affect the effectiveness of immune checkpoint inhibitors (95). In agreement with this hypothesis, our data showed that PD-1 blockade didn't significantly decrease tumor

number and tumor area in NNK-treated mice with persistent exposure to LPS. Nevertheless, selective elimination of GrMDSCs, which has been reported as the more suppressive subtype of MDSCs in the tumor microenvironment efficiently inhibits lung tumorigenesis (96). Furthermore, we observed that combined PD-1 blockade and MDSC depletion enhanced treatment efficacy compared to single treatment alone, which are supported by other studies (90, 97). These *in vivo* results may partly explain that a proportion of patients still has progression of disease after anti-PD-1 treatment despite high immune gene signature expression as seen in GSE93157 and other cohorts (47), suggesting the coexisting other inhibitory pathways or coinhibitory signals such as the presence of immunosuppressive cells (MDSCs and Tregs) in the tumor microenvironment. Therefore, removal of coinhibitory signals, such as MDSC depletion combined with checkpoint inhibitors, could improve treatment efficacy as seen in our model.

3.4 Summary

In summary, our findings demonstrated that LPS-mediated chronic inflammation in NNK-treated mice synergistically augmented lung tumorigenesis consistent with induction of an immunosuppressive microenvironment. In this instance, immunosuppression was characterized by MDSCs and Tregs accumulation, T-cell exhaustion, and increased PD-1/PD-L1 checkpoint pathway activities. PD-1 blockade demonstrated favorable treatment efficacy in inflammation-associated lung cancer in the NNK/LPS-treated mice. Moreover, the combined PD-1 blockade (by anti-PD-1 antibody treatment) and MDSC depletion (by anti-Ly6G treatment) were even more effective at inhibiting tumor formation in mice. These findings support the concept that PD-1 blockade combined with MSDC depletion could be a novel therapeutic approach for lung cancer

in the setting of chronic pulmonary inflammation, as is frequently present in patients with COPD. Furthermore, we identified valuable immune gene signatures associated with treatment responses and survival outcome in patients with NSCLC under either immunotherapy or conventional treatment, which forms the basis to use these immune gene signatures as potential biomarkers for clinical utility in existing or ongoing clinical trials for NSCLC treatment.

4.0 MMPS-Gene Signature Predicts Survival Outcome in Stage I Lung Adenocarcinoma

4.1 Introduction

Despite curative surgery for early-stage lung cancer, tumor recurrence remains the main causes of cancer-related death (11-14). It is estimated that 18.5% of patients with stage I lung adenocarcinoma after complete surgical resection have been reported to have cancer recurrence (98). It suggests that these patients with a higher risk of recurrence following surgery can't be distinguished by the current lung cancer staging system (15).

Although adjuvant chemotherapy has been shown to decrease tumor recurrence and prolong survival in completely resected stage II or III NSCLC, its role in stage I disease remains controversial (16-18, 99-102). Previous studies showed that patients with stage I disease didn't benefit from adjuvant chemotherapy after surgical resection except for survival advantage for stage IB patients who had tumor size ≥ 4cm (99). This is probably because patients with stage I disease and low-risk of recurrence may not get benefit from routine adjuvant chemotherapy. However, patients with high-risk factor such as large tumor size (≥ 4cm) demonstrated a significant survival difference in favor of adjuvant chemotherapy, which highlights the need of reliable prognostic biomarkers to stratify high-risk stage I disease for adjuvant chemotherapy.

Degradation of extracellular matrix and penetration of basement membrane have been shown to involve in tumor invasion and metastasis (103, 104). Studies have shown that the high levels of MMPs including MMP1, MMP2, MMP9, MMP10, and MMP12 were expressed in lung tumor and correlated with tumor recurrence and poor survival outcome in patients with surgically resected NSCLC (60, 61, 105-107). In addition, each MMP can degrade multiple substrates, and many substrates are degraded by multiple MMPs, suggesting that multiple MMPs may involve in either physiological processes or disease progression such as cancer (108). However, previous studies assessed individual MMP in predicting lung cancer prognosis showing inconsistent results

(62). In addition, their effects on survival outcome for stage I lung adenocarcinoma remain unknown.

To explore the MMPs expression in lung tumors, we analyzed two publicly available lung adenocarcinoma datasets and discovered MMPs-enriched gene clusters. An MMPs-gene signature was further identified from these two MMPs-gene clusters as a potential biomarker to predict survival outcome in patients with stage I lung adenocarcinoma after complete resection. Finally, we validated the prognostic transcriptome signature in an independent cohort. Our study provided a valuable biomarker to guide the use of adjuvant therapeutics for patients with early-stage lung cancer at high-risk of recurrence.

4.2 Results

4.2.1 Overview of this study

To determine whether expression of different MMPs in lung tumors could be potential prognostic biomarkers, we performed a series of analyses in multiple discovery and validation cohorts as diagrammed in Figure 14. We first analyzed two lung adenocarcinoma datasets of GSE31210 and TCGA as the discovery cohorts to identify MMPs-enriched gene clusters. The common genes between two MMPs-gene clusters were further identified as MMPs-associate gene signature. Finally, the utility of MMPs-gene signature to predict PFS and OS in stage I lung adenocarcinomas was examined in all datasets.

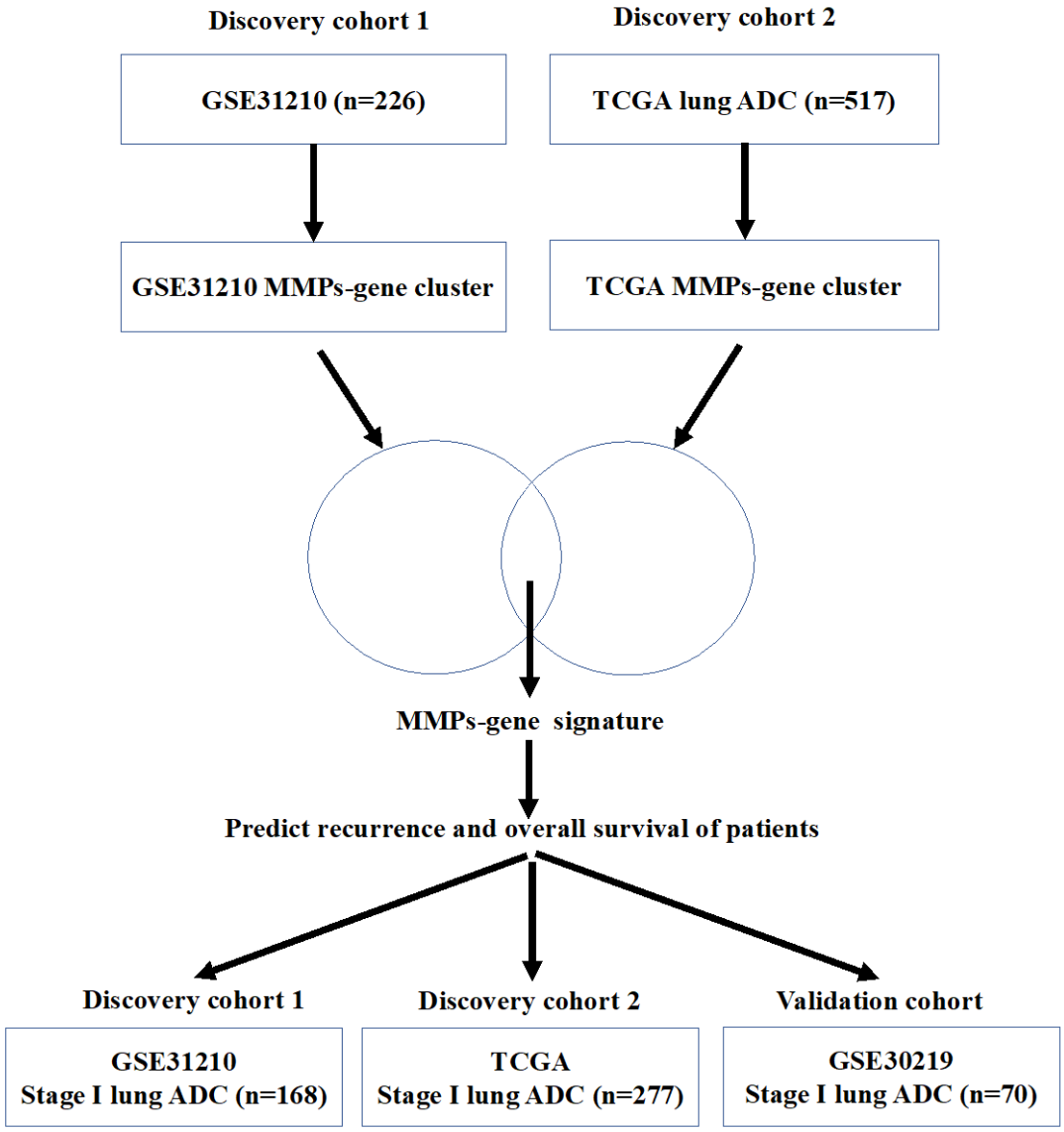

Figure 14. The schematic diagram of this study.

The discovery datasets including GSE31210 and TCGA lung ADC were used to define MMPs-gene clusters. The 36-gene MMPs signature was further identified and applied to patients with stage I lung adenocarcinoma after surgical resection for survival analysis in discovery and validation cohorts. ADC = adenocarcinoma.

4.2.2 Multiple MMPs co-express in lung tumors and correlate with poor survival outcome

In order to examine the MMPs expression in lung tumors, we analyzed gene expression of 226 lung adenocarcinoma samples and 20 normal lung samples from GSE31210 stage I-II lung adenocarcinoma cohort (Table 4). We performed unsupervised hierarchical clustering heatmap of differentially expressed genes (absolute fold change >2.5, FDR<0.05) between tumor and normal tissue (Figure 15A). The result showed that a 150-gene cluster with enriched MMPs including *MMP1, MMP3, MMP9, MMP11, MMP12, MMP13* and increased expression in tumors compared to normal tissue (Figure 15B). In addition, Ingenuity pathway analysis of the 150-gene cluster showed significant pathways all involving in MMPs (Figure 15 C). Unsupervised hierarchical clustering heatmap revealed four lung adenocarcinoma subgroups clustered with the 150-gene cluster (Figure 15D). Overall, the MMP-gene cluster expression from subgroup 1 to subgroup 4 was consistent with the expression pattern from low to high. In addition, patients with higher gene signature expression correlated with worse progression-free survival (PFS) and overall survival (OS) than those with lower expression (Figure 15E).

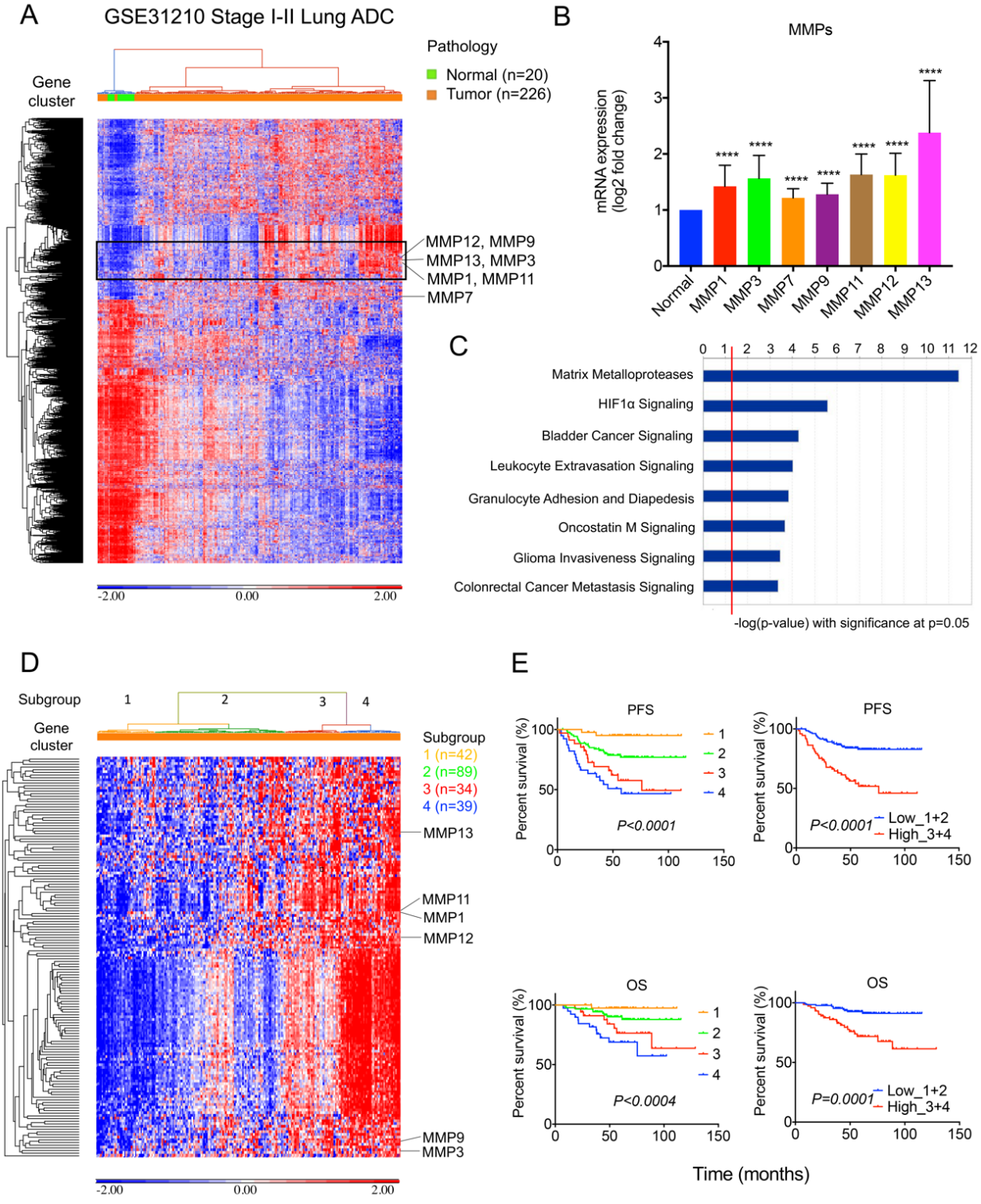
A
GSE31210 Stage I-II Lung ADC
Pathology
Normal (n=20)
Tumor (n=226)
Gene cluster
MMP12, MMP9
MMP13, MMP3
MMP1, MMP11
MMP7
-2.00
0.00
2.00
B
MMPs
mRNA expression (log2 fold change)
Normal
MMP1
MMP3
MMP7
MMP9
MMP11
MMP12
MMP13
C
Matrix Metalloproteases
HIF1α Signaling
Bladder Cancer Signaling
Leukocyte Extravasation Signaling
Granulocyte Adhesion and Diapedesis
Oncostatin M Signaling
Glioma Invasiveness Signaling
Colonrectal Cancer Metastasis Signaling
-log(p-value) with significance at p=0.05
D
Subgroup
Gene cluster
Subgroup
1 (n=42)
2 (n=89)
3 (n=34)
4 (n=39)
MMP13
MMP11
MMP1
MMP12
MMP9
MMP3
E
PFS
Percent survival (%)
P<0.0001
P<0.0001
Low_1+2
High_3+4
OS
P<0.0004
P=0.0001
Time (months)

Figure 15. MMPs-gene cluster increases expression in lung tumors and associated with survival outcome in GSE31210 cohort.

226 lung adenocarcinoma patient samples and 20 normal lung samples from the GSE31210 stage I-II lung adenocarcinoma cohort were analyzed. (A) Unsupervised hierarchical clustering heatmap of differentially expressed genes between tumor and normal lung tissue was performed. A 150-gene cluster with enriched MMPs was identified (square). (B) The MMPs including MMP1, MMP3, MMP7, MMP9, MMP11, MMP12, and MMP13 increased expression in tumors compared to normal lung tissue. Data shown are mean ± S.D. ****P < 0.0001 using one-way ANOVA. (C) Ingenuity pathway analysis of the 150-gene cluster showed significant pathways. (D) Unsupervised hierarchical clustering heatmap revealed four lung adenocarcinoma subgroups clustered with 150-gene cluster (E) Kaplan–Meier survival analysis of patient subgroups based on the 150-gene cluster were done using the log-rank test.

Table 4.Clinical Characteristics of GSE31210 Stage I-II Lung Adenocarcinoma Cohort.

Characteristics	***N* (%)**
Subjects, *n*	226
Sex, M/F, *n* (%)	105/121 (46/54)
Age, yr, mean ± SD	60 ± 7
pTNM stages	
IA	114 (50)
IB	54 (24)
II	58 (26)
Smoking status	
Non-smoker	115 (51)
Ever-smoker	111 (49)
Mutation status	
EGFR_MUT	127 (56)
KRAS_MUT	20 (9)
ALK _Fusion	11 (5)
KRAS/EGFR/AKL_WT	68 (30)
Exclude for prognosis analysis	22 (9.7)

Clinical–pathologic characteristics of GSE31210 lung adenocarcinoma cohort (n=226) were evaluated in this study. 22 cases were excluded for prognosis analysis due to incomplete resection or adjuvant therapy. *Definition of abbreviations:* ALK= Anaplastic lymphoma kinase; EGFR= epidermal growth factor receptor; MUT = mutation; pTNM stages = pathologic TNM stages of malignant tumors; WT = wild type.

4.2.3 Increased MMPs expression correlated with poor prognosis in an independent lung adenocarcinoma cohort

To validate the results form GSE31210 cohort, we performed a transcriptome analysis of TCGA lung adenocarcinoma cohort (Table 5), which included 517 lung tumor samples and 59 adjacent normal lung tissue samples. The unsupervised hierarchical clustering heatmap based on the differentially expressed genes (absolute fold change >2.5, FDR<0.05) between tumor and normal adjacent lung tissue (Figure 16A). Similarly, the result showed a 185-gene cluster with enriched MMPs including *MMP1, MMP3, MMP9, MMP10, MMP11, MMP12, MMP13* and increased expression in tumors than adjacent normal lung tissue (Figure 16B). Ingenuity pathway analysis of the 185-gene cluster revealed significant pathways mainly involving in MMPs (Figure 16C). Unsupervised hierarchical clustering heatmap revealed four lung adenocarcinoma subgroups clustered with the 185-gene cluster (Figure 16D). Similarly, patients with higher gene cluster expression correlated with worse PFS and OS than those with lower expression (Figure 16E).

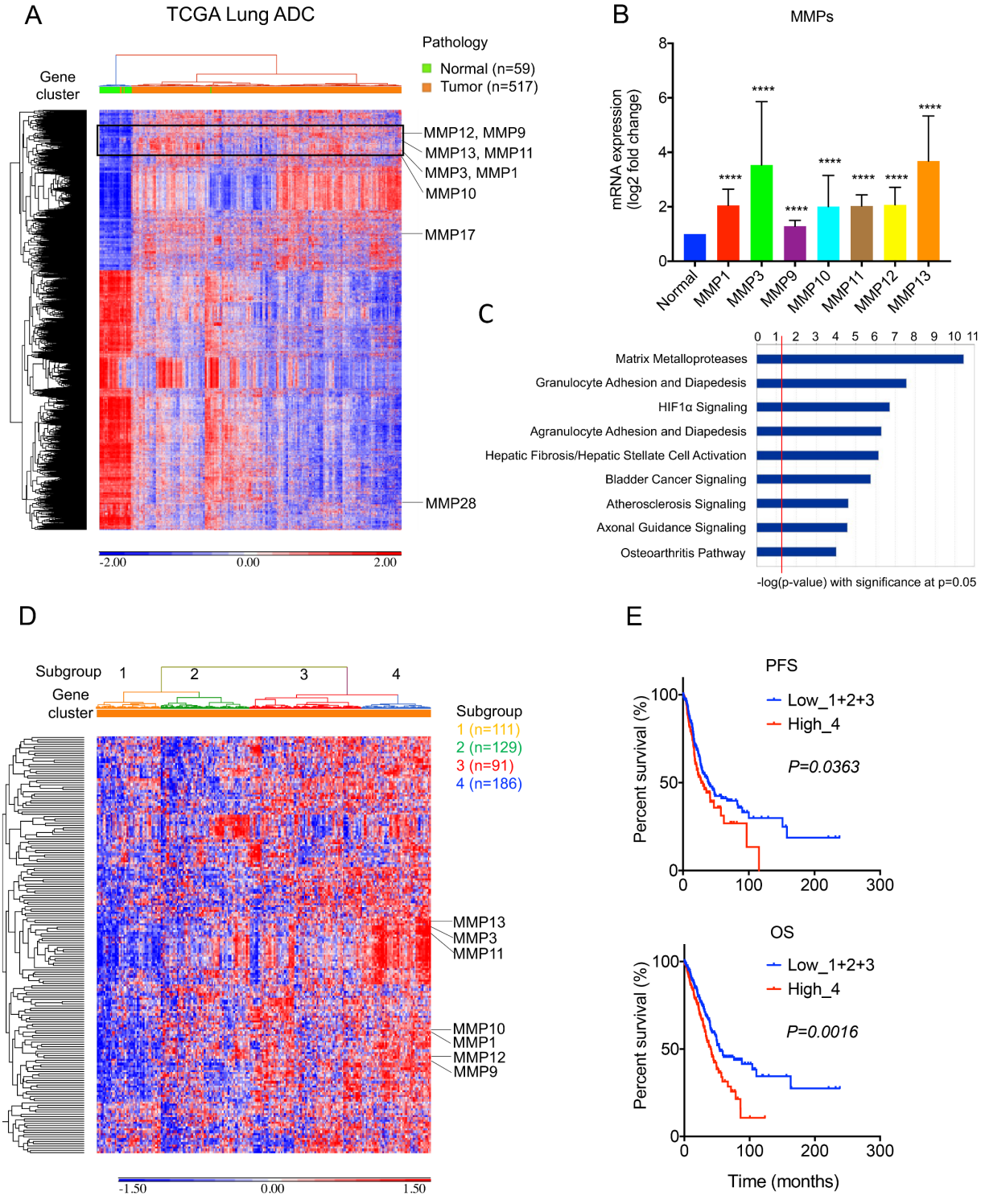
A
TCGA Lung ADC
Pathology
Normal (n=59)
Tumor (n=517)
Gene cluster
MMP12, MMP9
MMP13, MMP11
MMP3, MMP1
MMP10
MMP17
MMP28
-2.00
0.00
2.00
B
MMPs
mRNA expression (log2 fold change)
Normal
MMP1
MMP3
MMP9
MMP10
MMP11
MMP12
MMP13
C
Matrix Metalloproteases
Granulocyte Adhesion and Diapedesis
HIF1α Signaling
Agranulocyte Adhesion and Diapedesis
Hepatic Fibrosis/Hepatic Stellate Cell Activation
Bladder Cancer Signaling
Atherosclerosis Signaling
Axonal Guidance Signaling
Osteoarthritis Pathway
-log(p-value) with significance at p=0.05
D
Subgroup
Gene cluster
Subgroup
1 (n=111)
2 (n=129)
3 (n=91)
4 (n=186)
MMP13
MMP3
MMP11
MMP10
MMP1
MMP12
MMP9
-1.50
0.00
1.50
E
PFS
Low_1+2+3
High_4
P=0.0363
Percent survival (%)
OS
P=0.0016
Time (months)

Figure 16. MMPs increased expression in lung tumor and associated with survival outcome in TCGA cohort.

517 lung adenocarcinoma patient samples and 59 normal adjacent lung samples from the TCGA lung adenocarcinoma cohort were analyzed. (A) Unsupervised hierarchical clustering heatmap of differentially expressed genes between tumor and normal lung tissue was performed. A 185-gene cluster with enriched MMPs was identified (square). (B) The MMPs including MMP1, MMP3, MMP9, MMP11, MMP12, and MMP13 increased expression in tumors than normal lung tissue. Data shown are mean ± S.D. ****$P < 0.0001$ using one-way ANOVA. (C) Ingenuity pathway analysis of the 185-gene cluster showed significant pathways. (D) Unsupervised hierarchical clustering heatmap revealed four lung adenocarcinoma subgroups clustered with 185-gene cluster. (E) Kaplan–Meier survival analysis of patient subgroups based on 185-gene cluster was done using the log-rank test.

Table 5. Clinical Characteristics of TCGA Lung Adenocarcinoma Cohort.

Characteristics	*N* (%)
Subjects, *n*	517
Sex, M/F, *n* (%)	240/277 (46/54)
Age, yr, mean ± SD	65 ± 13
pTNM stages	
I	277 (54)
II	122 (24)
III	84 (16)
IV	26 (5)
NA	8 (1)
Smoking status	
Non-smoker	76 (15)
Ex-smoker	308 (60)
Current-smoker	119 (23)
NA	14 (2)
Mutation status	
EGFR_MUT	66 (13)
KRAS_MUT	154 (30)
ALK _Fusion	5 (1)
KRAS/EGFR/AKL_WT	285 (55)
NA	7 (1)
ECOG	
0	62 (12)
1	58 (11)
2	17 (3)
3	5 (1)
4	2 (1)
NA	373 (72)
Treatment	
Surgery	386 (75)
Radiotherapy	43 (8)
Chemotherapy	155 (30)
Targeted therapy	18 (3)
Primary therapy response	
CR	296 (57)
PR	6 (1)
SD	34 (7)
PD	65 (13)
NA	156 (22)

Clinical–pathologic characteristics of TCGA lung adenocarcinoma cohort (n=517) were evaluated in this study. *Definition of abbreviations:* ALK = Anaplastic lymphoma kinase; CR = complete response; ECOG = Eastern Cooperative Oncology Group; EGFR= epidermal growth factor receptor; MUT = mutation; NA = not applicable; PD = progression disease; PFS = progression-free survival; PR = partial response; SD = stable disease; pTNM stages = pathologic TNM stages of malignant tumors; TCGA = the cancer genome atlas; WT = wild type.

4.2.4 Development of a 36-gene MMP signature with a network analysis

To search for the common molecular signatures associated with MMPs in these two cohorts, we identified 36 overlapping genes, which contained MMPs and the co-expressed genes present in both MMPs-gene clusters of GSE31210 and TCGA cohort, termed 36-gene MMP signature (Figure 17A). Ingenuity pathway analysis of the 36-gene MMP signature showed multiple associated pathways with significance especially in the pathway related to MMPs (Figure 17B). The network analysis of 150-gene cluster from GSE31210 cohort showed the prediction of important upstream regulators such as MYBL2, E2F8, FOXM1, and FHL2 to transcriptionally regulate this interaction network (Figure 17C). In addition, the 185-gene cluster from the TCGA cohort revealed the connection of MAPK/ERK and NFκB pathway in the network (Figure 17D). Notably, the network analysis results showed the direct and indirect interaction between MMPs in both gene clusters, suggesting that these MMPS are functionally related molecules and involved in lung tumorigenesis (Figures 17C-D, square).

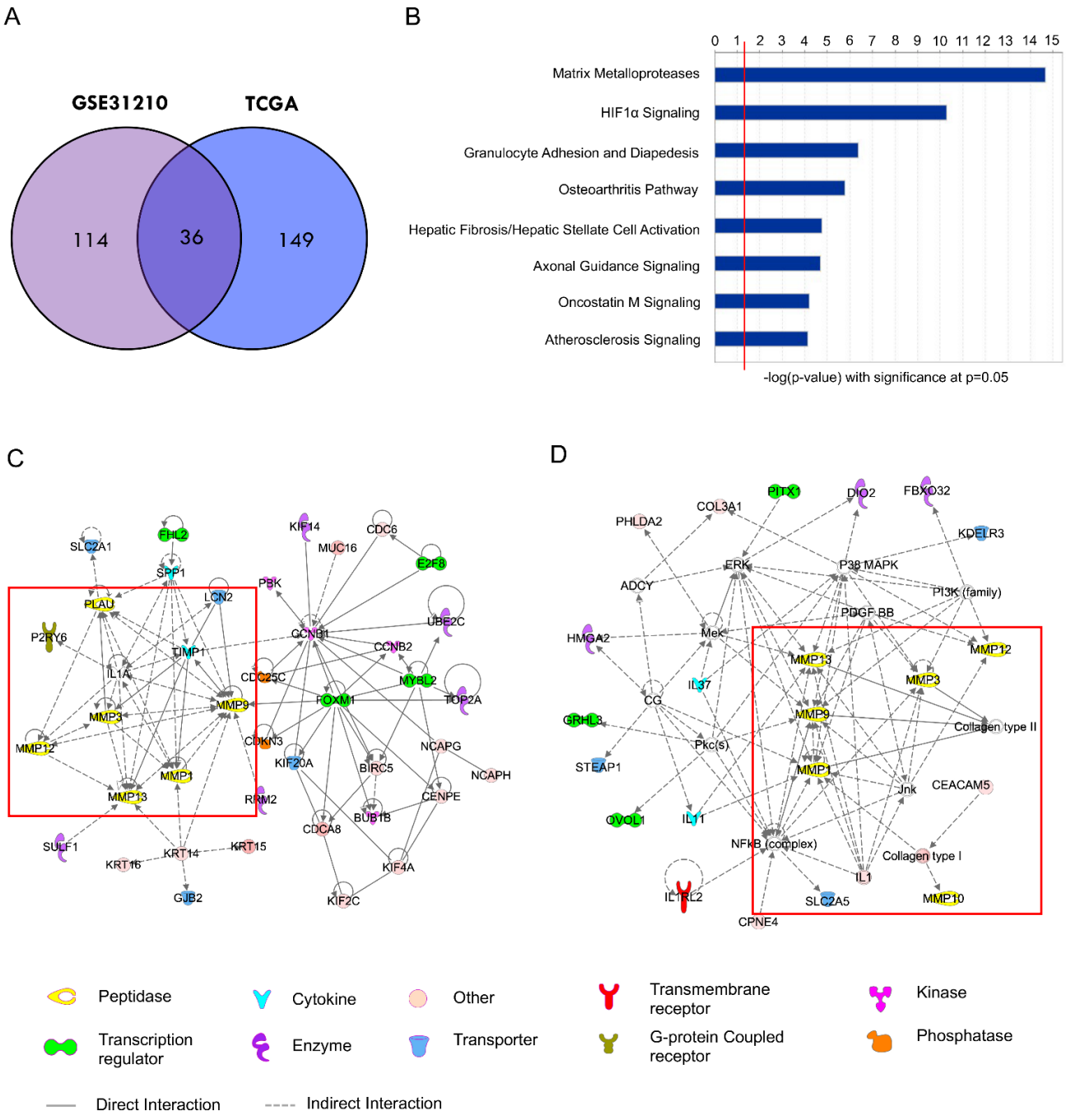

Figure 17. Characteristics of a 36-gene MMP signature and network analysis.

(A) Venn diagram showed 36 MMP-associated genes which were present in both MMPs-enriched gene clusters of GSE31210 and TCGA cohort. (B) Ingenuity pathway analysis of the 36-gene MMP signature showed pathways that are likely to be significantly involved. (C) Networks analysis of the 150-gene cluster from GSE31210 cohort. (D) Networks analysis of the 185-gene cluster from TCGA cohort.

4.2.5 The 36-gene MMP signature predicts poor survival outcome in GSE3120 stage I lung adenocarcinomas

To determine the prognostic value of the 36-gene MMP signature in stage I lung adenocarcinoma, we performed the unsupervised hierarchical clustering heatmap of the gene signature and stage I lung adenocarcinoma from GSE31210 cohort. The result revealed three lung adenocarcinoma subgroups clustered with the gene signature (Figure 18A). In survival analysis, patients with higher gene signature expression were associated with worse PFS and OS than those with lower expression (Figure 18B). Importantly, the patient cluster with increased MMPs-gene signature expression remained an independent risk factor for PFS and OS in patients with stage I lung adenocarcinoma after adjustments of stage, gender, age, smoking, and mutation status (Table 6). We also analyzed the gene mutation in these subgroups and the results revealed mutation status were differentially distributed between subgroups (Figure 18C). The patient subgroup with higher MMPs-gene signature expression showed a lower proportion of EGFR mutations but higher KRAS mutations and triple-negative mutations compared to those with lower expression (Figure 18C). Consistently, the GSEA showed that the 36-gene MMP signature enriched in EGFR wild type tumors, especially in KRAS-driven lung tumors (Figure 18D).

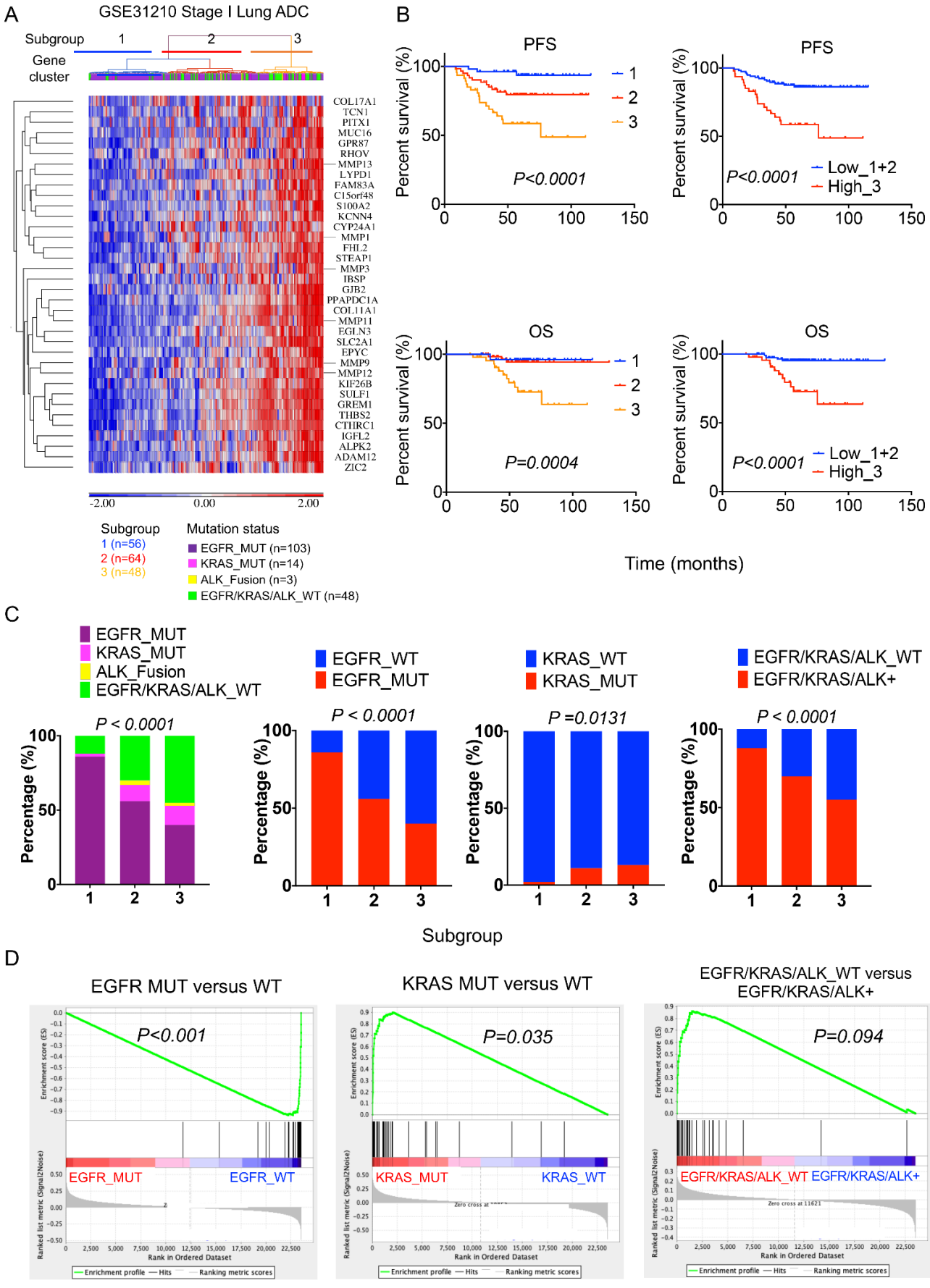
A
GSE31210 Stage I Lung ADC
Subgroup
Gene cluster
COL17A1
TCN1
PITX1
MUC16
GPR87
RHOV
MMP13
LYPD1
FAM83A
C15orf48
S100A2
KCNN4
CYP24A1
MMP1
FHL2
STEAP1
MMP3
IBSP
GJB2
PPAPDC1A
COL11A1
MMP11
EGLN3
SLC2A1
EPYC
MMP9
MMP12
KIF26B
SULF1
GREM1
THBS2
CTHRC1
IGFL2
ALPK2
ADAM12
ZIC2
-2.00
0.00
2.00
Subgroup
1 (n=56)
2 (n=64)
3 (n=48)
Mutation status
EGFR_MUT (n=103)
KRAS_MUT (n=14)
ALK_Fusion (n=3)
EGFR/KRAS/ALK_WT (n=48)
B
PFS
Percent survival (%)
P<0.0001
OS
P=0.0004
Low_1+2
High_3
Time (months)
C
EGFR_MUT
KRAS_MUT
ALK_Fusion
EGFR/KRAS/ALK_WT
P < 0.0001
Percentage (%)
EGFR_WT
EGFR_MUT
KRAS_WT
KRAS_MUT
P =0.0131
EGFR/KRAS/ALK+
Subgroup
D
EGFR MUT versus WT
KRAS MUT versus WT
EGFR/KRAS/ALK_WT versus EGFR/KRAS/ALK+
P<0.001
P=0.035
P=0.094
Enrichment score (ES)
Ranked list metric (Signal2Noise)
Rank in Ordered Dataset
Enrichment profile
Hits
Ranking metric scores

Figure 18. MMPs-gene signature predicts poor survival outcome in GSE31210 stage I lung adenocarcinoma.

168 stage I lung adenocarcinoma patient samples from the GSE31210 cohort were analyzed. (A) Unsupervised hierarchical clustering heatmap revealed three lung adenocarcinoma subgroups clustered with 36-gene MMP signature. (B) Kaplan–Meier survival analysis of patient subgroups based on the 36-gene MMP signature was done using the log-rank test. (C) The distribution difference among the three subgroups in mutation status was tested by the Chi-squared test. (D) GSEA showed the enrichment of 36-gene MMP signature based on mutation status in GSE31210 cohort.

.

Table 6. Univariate and Mutlivariate Analysis of Progression-free and Overall Survival in 162 stage I lung adenocarcinoma.

Variable	Progression-free Survival				Overall Survival			
	Univariate Analysis		Multivariate Analysis		Univariate Analysis		Multivariate Analysis	
	hazard ratio (95% CI)	*P value*	*hazard ratio (95% CI)*	*P value*	*hazard ratio (95% CI)*	*P value*	*hazard ratio (95% CI)*	*P value*
Sex, M	0.99 (0.50–1.96)	0.98	0.78 (0.33–1.83)	0.56	1.14 (0.43–3.07)	0.88	0.84 (0.23–3.03)	0.79
Age, per 1 yr*	1.01 (0.96–1.06)	0.67	0.99 (0.96–1.06)	0.68	0.99 (0.93–1.06)	0.73	0.97 (0.91–1.04)	0.38
Stage IB vs IA	3.02 (1.53–5.95)	0.001	2.18 (1.06–4.5)	**0.03**	2.16 (0.81–5.78)	0.12	1.25 (0.43–3.61)	0.68
Smoking status								
Ever-smoker vs. Never-smoker	1.06 (0.54–2.08)	0.87	0.93 (0.39–2.23)	0.86	1.46 (0.55–3.89)	0.45	1.11 (0.30–4.02)	0.88
Mutation status								
EGFR_MUT vs. KRAS/EGFR/AKL_WT	0.44 (0.22–0.92)	**0.029**	0.61 (0.29–1.28)	0.19	0.35 (0.13–0.96)	**0.042**	0.48 (0.17-1.40)	0.18
KRAS_MUT vs. KRAS/EGFR/AKL_WT	0.84 (0.28–2.55)	0.76	0.60 (0.19–1.91)	0.39	0.35 (0.04–2.80)	0.32	0.29 (0.04–2.42)	0.26
ALK _Fusion vs. KRAS/EGFR/AKL_WT	$9.40e^{-7}$ (0–Inf)	0.99	$1.27e^{-10}$ (0–Inf)	0.99	$6.37e^{-9}$ (0–Inf)	0.99	$1.44e^{-10}$ (0-Inf)	0.99
MMP gene signature								
High vs Low	3.89 (1.97–7.67)	**0.04**	3.14 (1.49–6.60)	**0.003**	6.43 (2.23–18.53)	**0.0006**	6.00 (1.92–18.72)	**0.002**

All variables were evaluated among the 162 patients with lung adenocarcinoma (6 patients excluded from 168 patients from GSE31210 cohort due to exclude for prognosis analysis due to incomplete resection or adjuvant therapy).

Factors associated with PFS and OS in univariate and multivariate Cox regression model (n=162 patients). The HR (95%CI) and *P* value are shown for each. *P* value <0.05 are set in bold for emphasis.

*Additional risk with each additional year of age.

Definition of abbreviations: ALK = Anaplastic lymphoma kinase; EGFR=epidermal growth factor receptor; Inf = Infinite; KRAS=Kirsten rat sarcoma 2 viral oncogene homolog; MMP=metalloproteinase; MUT=mutation; WT= wild type.

4.2.6 High 36-gene MMP signature expression predicts poor survival outcome in TCGA stage I lung adenocarcinomas

We further analyzed the TCGA stage I lung adenocarcinoma using the 36-gene MMP signature to re-evaluate the correlated prognosis. Unsupervised hierarchical clustering heatmap with the gene signature and stage I cases showed four lung adenocarcinoma subgroups (Figure 19A). In survival analysis, patients with higher MMP gene signature expression correlated with poor survival outcome than those with lower expression (Figure 19B). We also analyzed the gene mutation in these subgroups and the results revealed mutation status were differentially distributed between subgroups (Figure 19C). The patient subgroups with higher signature expression have a higher percentage of KRAS-mutant lung tumors (Figure 19C).

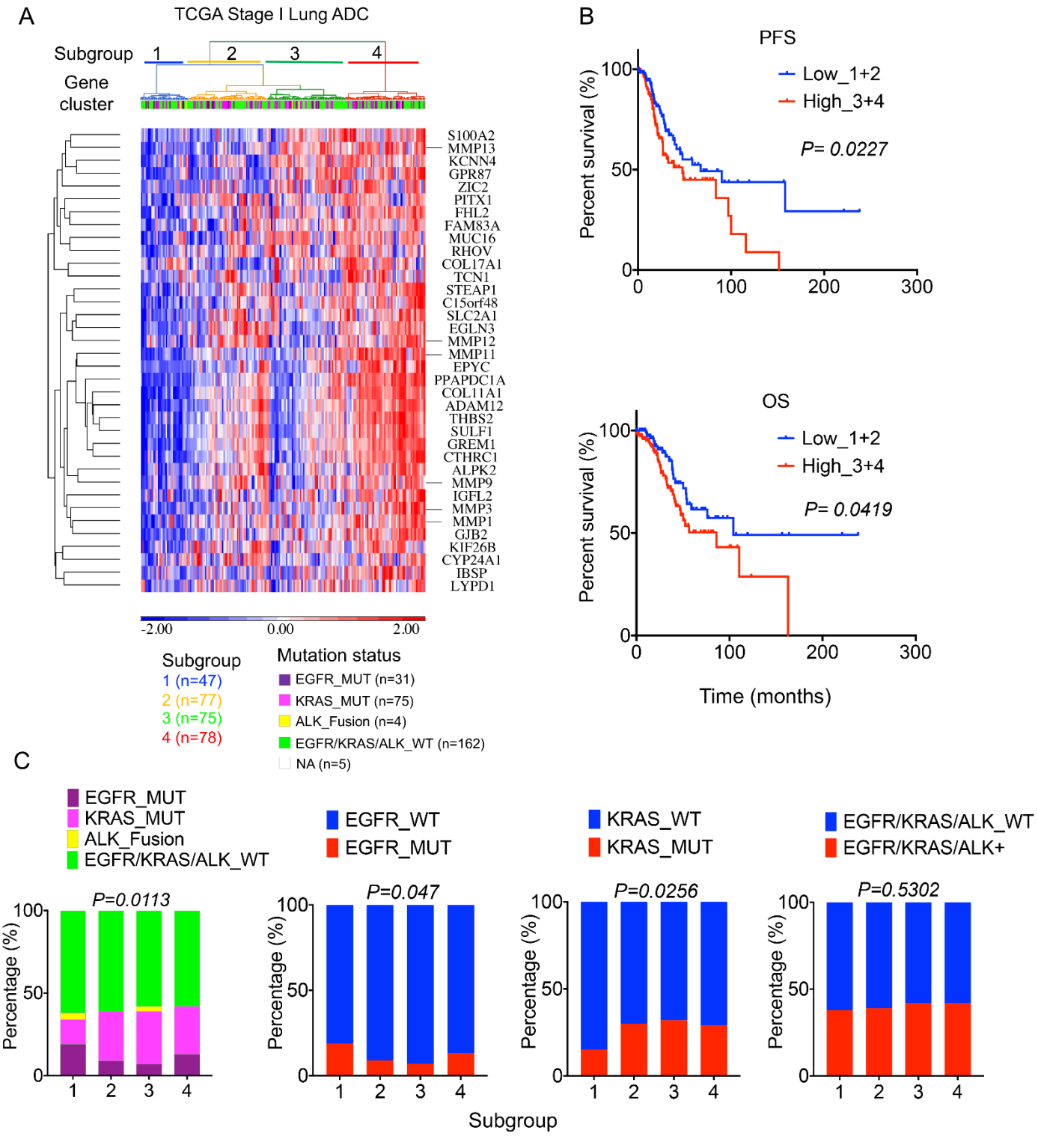
A
TCGA Stage I Lung ADC
Subgroup
1
2
3
4
Gene cluster
S100A2
MMP13
KCNN4
GPR87
ZIC2
PITX1
FHL2
FAM83A
MUC16
RHOV
COL17A1
TCN1
STEAP1
C15orf48
SLC2A1
EGLN3
MMP12
MMP11
EPYC
PPAPDC1A
COL11A1
ADAM12
THBS2
SULF1
GREM1
CTHRC1
ALPK2
MMP9
IGFL2
MMP3
MMP1
GJB2
KIF26B
CYP24A1
IBSP
LYPD1
-2.00
0.00
2.00
Subgroup
1 (n=47)
2 (n=77)
3 (n=75)
4 (n=78)
Mutation status
EGFR_MUT (n=31)
KRAS_MUT (n=75)
ALK_Fusion (n=4)
EGFR/KRAS/ALK_WT (n=162)
NA (n=5)
B
PFS
Low_1+2
High_3+4
P= 0.0227
Percent survival (%)
OS
P= 0.0419
Time (months)
C
EGFR_MUT
KRAS_MUT
ALK_Fusion
EGFR/KRAS/ALK_WT
P=0.0113
EGFR_WT
EGFR_MUT
P=0.047
KRAS_WT
KRAS_MUT
P=0.0256
EGFR/KRAS/ALK_WT
EGFR/KRAS/ALK+
P=0.5302
Percentage (%)
Subgroup

Figure 19. High MMPs-gene signature expression predicts poor survival outcome in TCGA stage I lung adenocarcinoma.

277 stage I lung adenocarcinoma patient samples from the TCGA cohort were analyzed. (A) Unsupervised hierarchical clustering heatmap revealed four lung adenocarcinoma subgroups clustered with 36-gene MMP signature. (B) Kaplan–Meier survival analysis of patient subgroups based on the 36-gene MMP signature done using the log-rank test. (C) The distribution difference among the four subgroups in mutation status was tested by the Chi-squared test.

4.2.7 The 36-gene MMP signature is validated in an independent lung cancer cohort

To validate the 36-gene MMP signature in an independent lung cancer cohort, we analyzed 70 stage I (T1N0M0) lung adenocarcinoma cases from GSE30219 cohort (Table 7). The 36-gene MMP gene signature was used for an unsupervised hierarchical clustering analysis on 70 stage I lung adenocarcinoma cases and the results suggested two distinct lung adenocarcinoma subgroups with high and low signature expression (Figure 20A). Consistently, patients with higher MMPs-gene signature expression correlated with worse PFS and OS compared those with lower expression (Figure 20B).

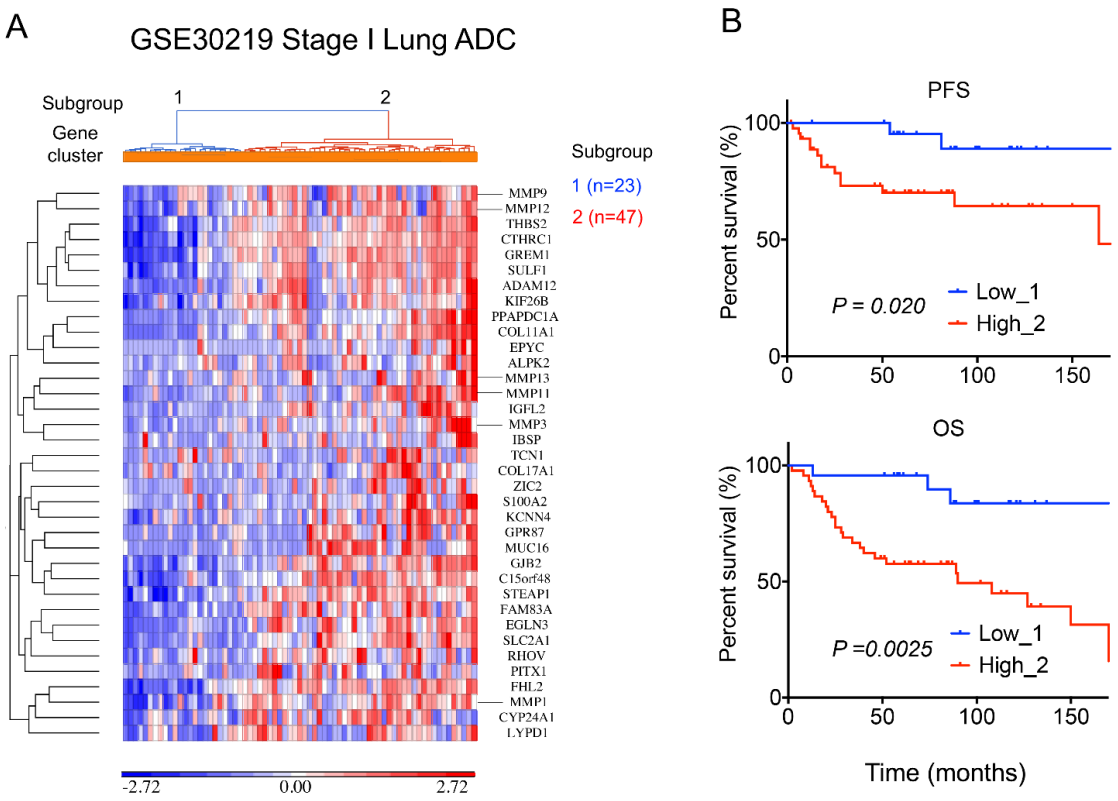

Figure 20. Validation of the 36-gene MMP signature in an independent GSE30219 lung cancer cohort.

70 stage I lung adenocarcinoma patient samples from the GSE30219 cohort were analyzed. (A) Unsupervised hierarchical clustering heatmap revealed two lung adenocarcinoma subgroups by clustering analysis using a 36-gene MMP signature. (B) Kaplan–Meier survival analysis of patient subgroups based on the 36-gene MMP signature was done using the log-rank test.

Table 7. Clinical Characteristics of GSE30219 Stage I Lung Adenocarcinoma Cohort.

Characteristics	***N* (%)**
Subjects, *n*	70
Sex, M/F, *n* (%)	54/16 (77/23)
Age, yr, mean ± SD	61 ± 9
pTNM stages	
T1N0M0	70 (100)
Tobacco	
Never-smoker	5 (7)
Former-smoker	34 (49)
Active-smoker	30 (43)
NA	1 (1)
TP53 mutation	
WT	42 (60)
MUT	25 (36)
NA	3 (4)
Adjuvant chemotherapy	
No	68 (97)
Yes	0 (0)
NA	2 (3)
Adjuvant radiotherapy	
No	69 (99)
Yes	0 (0)
NA	1 (1)

Clinical–pathologic characteristics of GSE30219 lung adenocarcinoma cohort (n=70) were evaluated in this study. *Definition of abbreviations:* MUT = mutation; NA = not applicable; pTNM stages = pathologic TNM stages of malignant tumors; WT = wild type.

4.3 Discussion

4.3.1 Multiple MMPs differentially co-express in lung tumors and correlate with worse survival outcome

Tumor recurrence after curative surgical resection poses a great challenge to the clinical management of early-stage NSCLC. Patients with stage I lung adenocarcinoma, which is the most histological subtype of NSCLC vary in survival outcome, suggesting the current staging system fails to stratify patient into subgroup based on the risk of recurrence. While several MMPs have been reported to correlate with recurrence and survival outcome in patients with surgically resected NSCLC, these results were not consistent in different studies (62). For instance, studies regarding the prognostic value of MMP-9 in blood or cancer tissue are contradictive, regardless of the detection technique. While several studies showed no prognostic value (109-113), others reported high MMP-9 expression correlated with poor prognosis (114-118). In addition, the prognostic value of MMPs in early-stage lung cancer, especially for stage I lung adenocarcinoma remains unclear. We hypothesized that various MMPs were differentially co-expressed in lung adenocarcinoma and have effects on worse survival outcome. Here, we performed unsupervised hierarchical clustering of DEGs between tumor and normal lung tissue in two lung adenocarcinoma cohorts. Our results showed MMPs-enriched gene clusters containing MMP1, MMP3, MMP9, MMP11, MMP12, and MMP13 in these two cohorts. Notably, these MMPs were clustered together and overexpressed in lung tumors compared to normal lung tissue, suggesting that they display similar gene expression pattern and may be functionally related during lung tumorigenesis. In consistent with this assumption, the network analysis also showed both direct and indirect interaction among MMPs and the related genes within the gene clusters. Therefore,

our results may partially explain the unsuccessful uses of individual MMP as a prognostic biomarker in predicting survival outcome because these studies probably overlooked the other co-expressed MMPs and the related molecules that led to inconsistent results (62). Adjuvant chemotherapy and radiotherapy have an effect on survival outcome and may affect survival analysis in surgically resected NSCLC. Therefore, we performed the survival analysis of patients with only stage I lung adenocarcinoma who received surgical resection without adjuvant chemotherapy or radiotherapy from GSE31210 and GSE30219 cohorts. Despite the incomplete data of adjuvant therapy after surgery in TCGA cohort, the result was consistent with other cohorts that the higher MMPs-gene signature expression associated with recurrence and poor overall survival in patients with surgically resected stage I lung adenocarcinoma.

4.3.2 MMPs-gene signature shows enrichment in KRAS-mutant lung tumors

Our results showed that the 36-gene MMPs signature displayed enrichment in EGFR-wild type lung tumors, especially in those with *KRAS* mutation compared to *ALK* translocation and triple negative mutations containing wild type *EGFR*, *KRAS*, and *ALK*, suggesting that these genes may be associated with *KRAS*-driven expression signature. A study has shown that patients with stage I lung adenocarcinoma and *KRAS* mutations have a significantly higher risk of recurrence than those without the mutation (119). In agreement, a recent meta-analysis suggested that *KRAS* mutations are associated with a poor survival outcome, especially in patients with lung adenocarcinoma and stage I disease (120). These findings may be partially explained by that the high MMPs-gene signature expression is associated with lung adenocarcinoma with *KRAS* mutations and correlated with recurrence and worse overall survival. In addition, the MMPs-gene signature also showed enrichment in triple negative lung tumors with a borderline statistical

difference, indicating the signature is not just limited to *KRAS* mutations. Despite the heterogenicity of mutations status such as higher EGFR mutation rate in GSE31210 cohort compared (61%) to TCGA cohort (11%) due to ethnicity, which is consistent with the Asians with higher EGFR mutation rate in lung adenocarcinoma such as GSE31210 cohort conducted in Japan (121), the MMPs-gene signature remained robustly predict survival outcome.

4.3.3 MMPs-gene signature is a potential prognostic biomarker

Several MMPs inhibitors (MMPIs) have been developed and used to treat various cancer types in clinical trials during the late 1990s and early 2000s (122-124). Even though the MMPIs showed promising effects in blocking tumor growth and metastasis in preclinical studies, clinical trials of these drugs were not successful (125-127). Several reasons have been hypothesized for the explanation including the difference between human and murine biology, the non-specificity of MMPIs, and the drug administration at an advanced stage. Preclinical testing reflected this concept that MMPIs successfully inhibited early-stage cancers and hematogenous metastases but had less effect on large tumors (126). It has been proposed that new trials should be designed to use MMPIs in patients with early-stage cancers and a high-risk of metastasis after surgery or as neoadjuvant therapy prior to surgery (128). The MMPs-gene signature may be useful for future clinical trials to identify patients with early-stage lung adenocarcinoma and high risk of recurrence for the MMPIs treatment after curative surgery.

4.4 Summary

In summary, we analyzed transcriptome data of lung adenocarcinoma cases in two discovery cohorts and identified MMPs-enriched gene clusters. A 36-gene MMPs signature was further selected, which successfully predicted the recurrence and worse overall survival in patients with stage I lung adenocarcinoma after curative surgery in discovery and validation cohorts. The MMPs-gene signature could be a potential biomarker for the proper stratification of early-stage lung cancer patients with a high risk of disease recurrence and worse overall survival for optimized follow-up schedule and the use of adjuvant therapeutics.

5.0 Conclusion

In the first part of the study, we established a murine lung cancer model by treating mice with tobacco carcinogen NNK and repeated LPS installation, which mimics the smoking carcinogen-induced, and COPD-like airway inflammation promoted lung cancer. Our findings demonstrated that LPS-mediated chronic inflammation in NNK-treated mice caused immunosuppressive microenvironment, characterized by MDSCs and Tregs accumulation, T cell exhaustion, and upregulated PD-1/PD-L1 checkpoint pathway. Furthermore, PD-1 blockade showed favorable treatment efficacy in inflammation-associated lung cancer such as NNK/LPS-treated mice compared to NNK-treated mice, and combined PD-1 blockade and MDSC depletion enhanced treatment efficacy. Lastly, we identified an overall immune gene signature, as well as the individual gene signatures of T-cell, B-cell, NK-cell, and Th1-cell, which could be potentially predictive and prognostic markers for NSCLC patients with immunotherapy or conventional treatments.

In the second part of the study, we analyzed transcriptome data of lung adenocarcinoma cases in two discovery cohorts and discovered MMPs-enriched gene clusters. A 36-gene MMPs signature was further identified, which showed enrichment in *KRAS*-mutant lung tumors and predicted recurrence and worse overall survival in patients with stage I lung adenocarcinoma after curative surgery in discovery and validation cohorts. These results will be important to identify early-stage patients with a high risk of disease recurrence for adjuvant therapeutics such as chemotherapy or MMPIs in future clinical trials.

6.0 Strength and Limitations

This study provides a comprehensive description of an inflammation-associated murine model of lung cancer induced by the synergistic action of tobacco smoke carcinogen and LPS, that is essential for understanding how inflammatory and immunosuppressive microenvironment contribute to the lung cancer progression. Our developed animal model also provides insights regarding the determinants of the PD-1 blockade efficacy in elevated inflammatory responses, and the depletion of myeloid-derived suppressor cells in significantly enhancing anti-PD-1 therapy efficacy. We identified valuable immune gene signatures successfully predict survival outcome of patients with NSCLC treated with either PD-1 blockade or conventional therapies. Furthermore, we are the first to use the clustering-based approach to identify MMPs-gene signature by the analysis of transcriptome profiling of lung adenocarcinoma cases. The MMPs-gene signature may be a potential biomarker to predict recurrence of patients with stage I lung adenocarcinoma after curative surgery and identify high-risk patients for adjuvant therapeutics in future trials.

Several limitations exist in this study. First, TLR4 is the receptor of LPS and widely expressed in lung epithelial cells and immune cells such as macrophages. The mechanism is not clear about whether the LPS is inducing upstream genomic alterations that are driving chemokine expression by tumor cells leading to increased tumor inflammation, or the LPS is simply inducing "non-specific" inflammation, and this inflammation is in some way contributing to tumorigenesis and tumor progression. Second, while the MDSCs depletion by anti-Ly6G treatment showed decreased lung tumors and enhanced anti-PD-1 treatment, the mechanism of anti-Ly6G mediated anti-tumor effect the combination with anti-PD-1 treatment is not clear. Third, the sample size of GSE93157 is small, and we didn't validate the immune gene signatures in other lung cancer

cohorts with immunotherapy due to the lack of other available public datasets. Fourth, these signature-based studies used different platforms, which may not be able to determine the optimal cut-off for the patient subgroup stratification.

More research is needed to determine the mechanism of LPS-mediated chronic inflammation in lung tumorigenesis using conditional TLR4-knockout mice constructed either in lung epithelial cells or myeloid cells. Furthermore, the transcriptome approach such as RNA-seq or Single-cell RNA-seq to analyzed mice treated with IgG control, anti-PD-1, anti-Ly6G or combined anti-PD-1 and Ly6G may be helpful for the hypothesis-generating studies to understand the mechanism of the effects of MDSCs depletion on lung tumorigenesis and immunotherapy. Finally, these potentially predictive and prognostic gene signatures need to be validated in a larger lung cancer cohort for clinical application.

Bibliography

1.Siegel RL, Miller KD, Jemal A. Cancer statistics, 2019. CA Cancer J Clin. 2019;69(1):7-34.

2.Molina JR, Yang P, Cassivi SD, Schild SE, Adjei AA. Non-small cell lung cancer: epidemiology, risk factors, treatment, and survivorship. Mayo Clin Proc. 2008;83(5):584-94.

3.Torre LA, Siegel RL, Jemal A. Lung Cancer Statistics. Adv Exp Med Biol. 2016;893:1-19.

4.Alberg AJ, Brock MV, Ford JG, Samet JM, Spivack SD. Epidemiology of lung cancer: Diagnosis and management of lung cancer, 3rd ed: American College of Chest Physicians evidence-based clinical practice guidelines. Chest. 2013;143(5 Suppl):e1S-e29S.

5.Subramanian J, Govindan R. Lung cancer in never smokers: a review. J Clin Oncol. 2007;25(5):561-70.

6.Doll R, Peto R. Mortality in relation to smoking: 20 years observations on male British doctors. Br Med J. 1976;2(6051):1525-36.

7.Straif K, Benbrahim-Tallaa L, Baan R, Grosse Y, Secretan B, El Ghissassi F, et al. A review of human carcinogens--Part C: metals, arsenic, dusts, and fibres. Lancet Oncol. 2009;10(5):453-4.

8.Driscoll T, Nelson DI, Steenland K, Leigh J, Concha-Barrientos M, Fingerhut M, et al. The global burden of disease due to occupational carcinogens. Am J Ind Med. 2005;48(6):419-31.

9.Humans IWGotEoCRt. Arsenic, metals, fibres, and dusts. IARC Monogr Eval Carcinog Risks Hum. 2012;100(Pt C):11-465.

10.Conway EM, Pikor LA, Kung SH, Hamilton MJ, Lam S, Lam WL, et al. Macrophages, Inflammation, and Lung Cancer. Am J Respir Crit Care Med. 2016;193(2):116-30.

11.Martini N, Bains MS, Burt ME, Zakowski MF, McCormack P, Rusch VW, et al. Incidence of local recurrence and second primary tumors in resected stage I lung cancer. J Thorac Cardiovasc Surg. 1995;109(1):120-9.

12.Harpole DH, Jr., Herndon JE, 2nd, Young WG, Jr., Wolfe WG, Sabiston DC, Jr. Stage I nonsmall cell lung cancer. A multivariate analysis of treatment methods and patterns of recurrence. Cancer. 1995;76(5):787-96.

13.al-Kattan K, Sepsas E, Fountain SW, Townsend ER. Disease recurrence after resection for stage I lung cancer. Eur J Cardiothorac Surg. 1997;12(3):380-4.

14.Nakagawa T, Okumura N, Ohata K, Igai H, Matsuoka T, Kameyama K. Postrecurrence survival in patients with stage I non-small cell lung cancer. Eur J Cardiothorac Surg. 2008;34(3):499-504.

15.Goldstraw P, Crowley J, Chansky K, Giroux DJ, Groome PA, Rami-Porta R, et al. The IASLC Lung Cancer Staging Project: proposals for the revision of the TNM stage groupings in the forthcoming (seventh) edition of the TNM Classification of malignant tumours. J Thorac Oncol. 2007;2(8):706-14.

16.Bradbury P, Sivajohanathan D, Chan A, Kulkarni S, Ung Y, Ellis PM. Postoperative Adjuvant Systemic Therapy in Completely Resected Non-Small-Cell Lung Cancer: A Systematic Review. Clin Lung Cancer. 2017;18(3):259-73 e8.

17.Arriagada R, Bergman B, Dunant A, Le Chevalier T, Pignon JP, Vansteenkiste J, et al. Cisplatin-based adjuvant chemotherapy in patients with completely resected non-small-cell lung cancer. N Engl J Med. 2004;350(4):351-60.

18.Winton T, Livingston R, Johnson D, Rigas J, Johnston M, Butts C, et al. Vinorelbine plus cisplatin vs. observation in resected non-small-cell lung cancer. N Engl J Med. 2005;352(25):2589-97.

19.Douillard JY, Rosell R, De Lena M, Carpagnano F, Ramlau R, Gonzales-Larriba JL, et al. Adjuvant vinorelbine plus cisplatin versus observation in patients with completely resected stage IB-IIIA non-small-cell lung cancer (Adjuvant Navelbine International Trialist Association [ANITA]): a randomised controlled trial. Lancet Oncol. 2006;7(9):719-27.

20.Solomon BJ, Mok T, Kim DW, Wu YL, Nakagawa K, Mekhail T, et al. First-line crizotinib versus chemotherapy in ALK-positive lung cancer. N Engl J Med. 2014;371(23):2167-77.

21.Mok TS, Wu YL, Thongprasert S, Yang CH, Chu DT, Saijo N, et al. Gefitinib or carboplatin-paclitaxel in pulmonary adenocarcinoma. N Engl J Med. 2009;361(10):947-57.

22.Herbst RS, Morgensztern D, Boshoff C. The biology and management of non-small cell lung cancer. Nature. 2018;553(7689):446-54.

23.Camidge DR, Pao W, Sequist LV. Acquired resistance to TKIs in solid tumours: learning from lung cancer. Nat Rev Clin Oncol. 2014;11(8):473-81.

24.Lievense LA, Sterman DH, Cornelissen R, Aerts JG. Checkpoint Blockade in Lung Cancer and Mesothelioma. Am J Respir Crit Care Med. 2017;196(3):274-82.

25.Gettinger S, Choi J, Hastings K, Truini A, Datar I, Sowell R, et al. Impaired HLA Class I Antigen Processing and Presentation as a Mechanism of Acquired Resistance to Immune Checkpoint Inhibitors in Lung Cancer. Cancer Discov. 2017;7(12):1420-35.

26.Zaretsky JM, Garcia-Diaz A, Shin DS, Escuin-Ordinas H, Hugo W, Hu-Lieskovan S, et al. Mutations Associated with Acquired Resistance to PD-1 Blockade in Melanoma. N Engl J Med. 2016;375(9):819-29.

27.Holmgaard RB, Zamarin D, Munn DH, Wolchok JD, Allison JP. Indoleamine 2,3-dioxygenase is a critical resistance mechanism in antitumor T cell immunotherapy targeting CTLA-4. J Exp Med. 2013;210(7):1389-402.

28.Allavena P, Garlanda C, Borrello MG, Sica A, Mantovani A. Pathways connecting inflammation and cancer. Curr Opin Genet Dev. 2008;18(1):3-10.

29.Mantovani A, Allavena P, Sica A, Balkwill F. Cancer-related inflammation. Nature. 2008;454(7203):436-44.

30.Du C, Wang Y. The immunoregulatory mechanisms of carcinoma for its survival and development. J Exp Clin Cancer Res. 2011;30:12.

31.Wang D, DuBois RN. Immunosuppression associated with chronic inflammation in the tumor microenvironment. Carcinogenesis. 2015;36(10):1085-93.

32.Siegel R, Ma J, Zou Z, Jemal A. Cancer statistics, 2014. CA Cancer J Clin. 2014;64(1):9-29.

33.Minino AM, Murphy SL, Xu J, Kochanek KD. Deaths: final data for 2008. Natl Vital Stat Rep. 2011;59(10):1-126.

34.Houghton AM. Mechanistic links between COPD and lung cancer. Nature reviews Cancer. 2013;13(4):233-45.

35.Mannino DM, Aguayo SM, Petty TL, Redd SC. Low lung function and incident lung cancer in the United States: data From the First National Health and Nutrition Examination Survey follow-up. Arch Intern Med. 2003;163(12):1475-80.

36.Koshiol J, Rotunno M, Consonni D, Pesatori AC, De Matteis S, Goldstein AM, et al. Chronic obstructive pulmonary disease and altered risk of lung cancer in a population-based case-control study. PLoS One. 2009;4(10):e7380.

37.Desai H, Eschberger K, Wrona C, Grove L, Agrawal A, Grant B, et al. Bacterial colonization increases daily symptoms in patients with chronic obstructive pulmonary disease. Ann Am Thorac Soc. 2014;11(3):303-9.

38.Patel IS, Seemungal TA, Wilks M, Lloyd-Owen SJ, Donaldson GC, Wedzicha JA. Relationship between bacterial colonisation and the frequency, character, and severity of COPD exacerbations. Thorax. 2002;57(9):759-64.

39.Pera T, Zuidhof A, Valadas J, Smit M, Schoemaker RG, Gosens R, et al. Tiotropium inhibits pulmonary inflammation and remodelling in a guinea pig model of COPD. Eur Respir J. 2011;38(4):789-96.

40.Diakos CI, Charles KA, McMillan DC, Clarke SJ. Cancer-related inflammation and treatment effectiveness. Lancet Oncol. 2014;15(11):e493-503.

41.Borghaei H, Paz-Ares L, Horn L, Spigel DR, Steins M, Ready NE, et al. Nivolumab versus Docetaxel in Advanced Nonsquamous Non-Small-Cell Lung Cancer. N Engl J Med. 2015;373(17):1627-39.

42.Brahmer J, Reckamp KL, Baas P, Crino L, Eberhardt WE, Poddubskaya E, et al. Nivolumab versus Docetaxel in Advanced Squamous-Cell Non-Small-Cell Lung Cancer. N Engl J Med. 2015;373(2):123-35.

43.Biton J, Ouakrim H, Dechartres A, Alifano M, Mansuet-Lupo A, Si H, et al. Impaired Tumor-Infiltrating T Cells in Patients with Chronic Obstructive Pulmonary Disease Impact Lung Cancer Response to PD-1 Blockade. Am J Respir Crit Care Med. 2018;198(7):928-40.

44.Mark NM, Kargl J, Busch SE, Yang GHY, Metz HE, Zhang H, et al. Chronic Obstructive Pulmonary Disease Alters Immune Cell Composition and Immune Checkpoint Inhibitor Efficacy in Non-Small Cell Lung Cancer. Am J Respir Crit Care Med. 2018;197(3):325-36.

45.Shukuya T, Carbone DP. Predictive Markers for the Efficacy of Anti-PD-1/PD-L1 Antibodies in Lung Cancer. J Thorac Oncol. 2016;11(7):976-88.

46.Nirmal AJ, Regan T, Shih BB, Hume DA, Sims AH, Freeman TC. Immune Cell Gene Signatures for Profiling the Microenvironment of Solid Tumors. Cancer Immunol Res. 2018;6(11):1388-400.

47.Ayers M, Lunceford J, Nebozhyn M, Murphy E, Loboda A, Kaufman DR, et al. IFN-gamma-related mRNA profile predicts clinical response to PD-1 blockade. The Journal of clinical investigation. 2017;127(8):2930-40.

48.Ji RR, Chasalow SD, Wang L, Hamid O, Schmidt H, Cogswell J, et al. An immune-active tumor microenvironment favors clinical response to ipilimumab. Cancer Immunol Immunother. 2012;61(7):1019-31.

49.Fehrenbacher L, Spira A, Ballinger M, Kowanetz M, Vansteenkiste J, Mazieres J, et al. Atezolizumab versus docetaxel for patients with previously treated non-small-cell lung cancer (POPLAR): a multicentre, open-label, phase 2 randomised controlled trial. Lancet. 2016;387(10030):1837-46.

50.Chen PL, Roh W, Reuben A, Cooper ZA, Spencer CN, Prieto PA, et al. Analysis of Immune Signatures in Longitudinal Tumor Samples Yields Insight into Biomarkers of Response and Mechanisms of Resistance to Immune Checkpoint Blockade. Cancer Discov. 2016;6(8):827-37.

51.Prat A, Navarro A, Pare L, Reguart N, Galvan P, Pascual T, et al. Immune-Related Gene Expression Profiling After PD-1 Blockade in Non-Small Cell Lung Carcinoma, Head and Neck Squamous Cell Carcinoma, and Melanoma. Cancer Res. 2017;77(13):3540-50.

52.Dufour A, Overall CM. Missing the target: matrix metalloproteinase antitargets in inflammation and cancer. Trends Pharmacol Sci. 2013;34(4):233-42.

53.DArmiento J, Dalal SS, Okada Y, Berg RA, Chada K. Collagenase expression in the lu ngs of transgenic mice causes pulmonary emphysema. Cell. 1992;71(6):955-61.

54.Vignola AM, Riccobono L, Mirabella A, Profita M, Chanez P, Bellia V, et al. Sputum metalloproteinase-9/tissue inhibitor of metalloproteinase-1 ratio correlates with airflow obstruction in asthma and chronic bronchitis. Am J Respir Crit Care Med. 1998;158(6):1945-50.

55.Hautamaki RD, Kobayashi DK, Senior RM, Shapiro SD. Requirement for macrophage elastase for cigarette smoke-induced emphysema in mice. Science. 1997;277(5334):2002-4.

56.Merchant N, Nagaraju GP, Rajitha B, Lammata S, Jella KK, Buchwald ZS, et al. Matrix metalloproteinases: their functional role in lung cancer. Carcinogenesis. 2017;38(8):766-80.

57.Egeblad M, Werb Z. New functions for the matrix metalloproteinases in cancer progression. Nature reviews Cancer. 2002;2(3):161-74.

58.Dreymueller D, Theodorou K, Donners M, Ludwig A. Fine Tuning Cell Migration by a Disintegrin and Metalloproteinases. Mediators Inflamm. 2017;2017:9621724.

59.Herbst RS, Yano S, Kuniyasu H, Khuri FR, Bucana CD, Guo F, et al. Differential expression of E-cadherin and type IV collagenase genes predicts outcome in patients with stage I non-small cell lung carcinoma. Clin Cancer Res. 2000;6(3):790-7.

60.Hofmann HS, Hansen G, Richter G, Taege C, Simm A, Silber RE, et al. Matrix metalloproteinase-12 expression correlates with local recurrence and metastatic disease in non-small cell lung cancer patients. Clin Cancer Res. 2005;11(3):1086-92.

61.Cho NH, Hong KP, Hong SH, Kang S, Chung KY, Cho SH. MMP expression profiling in recurred stage IB lung cancer. Oncogene. 2004;23(3):845-51.

62.Hadler-Olsen E, Winberg JO, Uhlin-Hansen L. Matrix metalloproteinases in cancer: their value as diagnostic and prognostic markers and therapeutic targets. Tumour Biol. 2013;34(4):2041-51.

63.Keohavong P, Kahkonen B, Kinchington E, Yin J, Jin J, Liu X, et al. K-ras mutations in lung tumors from NNK-treated mice with lipopolysaccharide-elicited lung inflammation. Anticancer Res. 2011;31(9):2877-82.

64.Newman AM, Liu CL, Green MR, Gentles AJ, Feng W, Xu Y, et al. Robust enumeration of cell subsets from tissue expression profiles. Nat Methods. 2015;12(5):453-7.

65.Becht E, Giraldo NA, Lacroix L, Buttard B, Elarouci N, Petitprez F, et al. Estimating the population abundance of tissue-infiltrating immune and stromal cell populations using gene expression. Genome Biol. 2016;17(1):218.

66.Abbas AR, Baldwin D, Ma Y, Ouyang W, Gurney A, Martin F, et al. Immune response in silico (IRIS): immune-specific genes identified from a compendium of microarray expression data. Genes Immun. 2005;6(4):319-31.

67.Abbas AR, Wolslegel K, Seshasayee D, Modrusan Z, Clark HF. Deconvolution of blood microarray data identifies cellular activation patterns in systemic lupus erythematosus. PLoS One. 2009;4(7):e6098.

68.Angelova M, Charoentong P, Hackl H, Fischer ML, Snajder R, Krogsdam AM, et al. Characterization of the immunophenotypes and antigenomes of colorectal cancers reveals distinct tumor escape mechanisms and novel targets for immunotherapy. Genome Biol. 2015;16:64.

69.Watkins NA, Gusnanto A, de Bono B, De S, Miranda-Saavedra D, Hardie DL, et al. A HaemAtlas: characterizing gene expression in differentiated human blood cells. Blood. 2009;113(19):e1-9.

70.Bindea G, Mlecnik B, Tosolini M, Kirilovsky A, Waldner M, Obenauf AC, et al. Spatiotemporal dynamics of intratumoral immune cells reveal the immune landscape in human cancer. Immunity. 2013;39(4):782-95.

71.Rutz S, Noubade R, Eidenschenk C, Ota N, Zeng W, Zheng Y, et al. Transcription factor c-Maf mediates the TGF-beta-dependent suppression of IL-22 production in T(H)17 cells. Nature immunology. 2011;12(12):1238-45.

72.Nikitin AY, Alcaraz A, Anver MR, Bronson RT, Cardiff RD, Dixon D, et al. Classification of proliferative pulmonary lesions of the mouse: recommendations of the mouse models of human cancers consortium. Cancer Res. 2004;64(7):2307-16.

73.Okayama H, Kohno T, Ishii Y, Shimada Y, Shiraishi K, Iwakawa R, et al. Identification of genes upregulated in ALK-positive and EGFR/KRAS/ALK-negative lung adenocarcinomas. Cancer Res. 2012;72(1):100-11.

74.Rousseaux S, Debernardi A, Jacquiau B, Vitte AL, Vesin A, Nagy-Mignotte H, et al. Ectopic activation of germline and placental genes identifies aggressive metastasis-prone lung cancers. Sci Transl Med. 2013;5(186):186ra66.

75.Malhotra J, Malvezzi M, Negri E, La Vecchia C, Boffetta P. Risk factors for lung cancer worldwide. Eur Respir J. 2016;48(3):889-902.

76.Young RP, Hopkins RJ, Christmas T, Black PN, Metcalf P, Gamble GD. COPD prevalence is increased in lung cancer, independent of age, sex and smoking history. Eur Respir J. 2009;34(2):380-6.

77.Young RP, Duan F, Chiles C, Hopkins RJ, Gamble GD, Greco EM, et al. Airflow Limitation and Histology Shift in the National Lung Screening Trial. The NLST-ACRIN Cohort Substudy. Am J Respir Crit Care Med. 2015;192(9):1060-7.

78.Crusz SM, Balkwill FR. Inflammation and cancer: advances and new agents. Nat Rev Clin Oncol. 2015;12(10):584-96.

79.Bronte V, Brandau S, Chen SH, Colombo MP, Frey AB, Greten TF, et al. Recommendations for myeloid-derived suppressor cell nomenclature and characterization standards. Nat Commun. 2016;7:12150.

80.Wherry EJ, Kurachi M. Molecular and cellular insights into T cell exhaustion. Nat Rev Immunol. 2015;15(8):486-99.

81.Moghaddam SJ, Li H, Cho SN, Dishop MK, Wistuba, II, Ji L, et al. Promotion of lung carcinogenesis by chronic obstructive pulmonary disease-like airway inflammation in a K-ras-induced mouse model. Am J Respir Cell Mol Biol. 2009;40(4):443-53.

82.Takahashi H, Ogata H, Nishigaki R, Broide DH, Karin M. Tobacco smoke promotes lung tumorigenesis by triggering IKKbeta- and JNK1-dependent inflammation. Cancer Cell. 2010;17(1):89-97.

83.Melkamu T, Qian X, Upadhyaya P, OSullivan MG, Kassie F. Lipopolysac charide enhances mouse lung tumorigenesis: a model for inflammation-driven lung cancer. Veterinary pathology. 2013;50(5):895-902.

84.You M, Candrian U, Maronpot RR, Stoner GD, Anderson MW. Activation of the Ki-ras protooncogene in spontaneously occurring and chemically induced lung tumors of the strain A mouse. Proc Natl Acad Sci U S A. 1989;86(9):3070-4.

85.Liu J, Hamrouni A, Wolowiec D, Coiteux V, Kuliczkowski K, Hetuin D, et al. Plasma cells from multiple myeloma patients express B7-H1 (PD-L1) and increase expression after stimulation with IFN-{gamma} and TLR ligands via a MyD88-, TRAF6-, and MEK-dependent pathway. Blood. 2007;110(1):296-304.

86.Taube JM, Anders RA, Young GD, Xu H, Sharma R, McMiller TL, et al. Colocalization of inflammatory response with B7-h1 expression in human melanocytic lesions supports an adaptive resistance mechanism of immune escape. Sci Transl Med. 2012;4(127):127ra37.

87.Trujillo JA, Sweis RF, Bao R, Luke JJ. T Cell-Inflamed versus Non-T Cell-Inflamed Tumors: A Conceptual Framework for Cancer Immunotherapy Drug Development and Combination Therapy Selection. Cancer Immunol Res. 2018;6(9):990-1000.

88.Akbay EA, Koyama S, Liu Y, Dries R, Bufe LE, Silkes M, et al. Interleukin-17A Promotes Lung Tumor Progression through Neutrophil Attraction to Tumor Sites and Mediating Resistance to PD-1 Blockade. J Thorac Oncol. 2017;12(8):1268-79.

89.Galon J, Bruni D. Approaches to treat immune hot, altered and cold tumours with combination immunotherapies. Nat Rev Drug Discov. 2019;18(3):197-218.

90.Highfill SL, Cui Y, Giles AJ, Smith JP, Zhang H, Morse E, et al. Disruption of CXCR2-mediated MDSC tumor trafficking enhances anti-PD1 efficacy. Sci Transl Med. 2014;6(237):237ra67.

91.Gabrilovich DI, Ostrand-Rosenberg S, Bronte V. Coordinated regulation of myeloid cells by tumours. Nat Rev Immunol. 2012;12(4):253-68.

92.Chang SH, Mirabolfathinejad SG, Katta H, Cumpian AM, Gong L, Caetano MS, et al. T helper 17 cells play a critical pathogenic role in lung cancer. Proc Natl Acad Sci U S A. 2014;111(15):5664-9.

93.Jin C, Lagoudas GK, Zhao C, Bullman S, Bhutkar A, Hu B, et al. Commensal Microbiota Promote Lung Cancer Development via gammadelta T Cells. Cell. 2019;176(5):998-1013 e16.

94.Serafini P, Mgebroff S, Noonan K, Borrello I. Myeloid-derived suppressor cells promote cross-tolerance in B-cell lymphoma by expanding regulatory T cells. Cancer Res. 2008;68(13):5439-49.

95.Whiteside TL, Demaria S, Rodriguez-Ruiz ME, Zarour HM, Melero I. Emerging Opportunities and Challenges in Cancer Immunotherapy. Clin Cancer Res. 2016;22(8):1845-55.

96.Maenhout SK, Van Lint S, Emeagi PU, Thielemans K, Aerts JL. Enhanced suppressive capacity of tumor-infiltrating myeloid-derived suppressor cells compared with their peripheral counterparts. International journal of cancer Journal international du cancer. 2014;134(5):1077-90.

97.Clavijo PE, Moore EC, Chen J, Davis RJ, Friedman J, Kim Y, et al. Resistance to CTLA-4 checkpoint inhibition reversed through selective elimination of granulocytic myeloid cells. Oncotarget. 2017;8(34):55804-20.

98.Yoshizawa A, Motoi N, Riely GJ, Sima CS, Gerald WL, Kris MG, et al. Impact of proposed IASLC/ATS/ERS classification of lung adenocarcinoma: prognostic subgroups and implications for further revision of staging based on analysis of 514 stage I cases. Mod Pathol. 2011;24(5):653-64.

99.Strauss GM, Herndon JE, 2nd, Maddaus MA, Johnstone DW, Johnson EA, Harpole DH, et al. Adjuvant paclitaxel plus carboplatin compared with observation in stage IB non-small-cell lung cancer: CALGB 9633 with the Cancer and Leukemia Group B, Radiation Therapy Oncology Group, and North Central Cancer Treatment Group Study Groups. J Clin Oncol. 2008;26(31):5043-51.

100.Butts CA, Ding K, Seymour L, Twumasi-Ankrah P, Graham B, Gandara D, et al. Randomized phase III trial of vinorelbine plus cisplatin compared with observation in completely resected stage IB and II non-small-cell lung cancer: updated survival analysis of JBR-10. J Clin Oncol. 2010;28(1):29-34.

101.Alam N, Darling G, Evans WK, Mackay JA, Shepherd FA, Lung Cancer Disease Site Group of Cancer Care Ontarios Program in Evidence -Based C. Adjuvant chemotherapy for completely resected non-small cell lung cancer: a systematic review. Crit Rev Oncol Hematol. 2006;58(2):146-55.

102.Wakelee HA, Dahlberg SE, Keller SM, Tester WJ, Gandara DR, Graziano SL, et al. Adjuvant chemotherapy with or without bevacizumab in patients with resected non-small-cell lung cancer (E1505): an open-label, multicentre, randomised, phase 3 trial. Lancet Oncol. 2017;18(12):1610-23.

103.Kleiner DE, Stetler-Stevenson WG. Matrix metalloproteinases and metastasis. Cancer Chemother Pharmacol. 1999;43 Suppl:S42-51.

104.Stamenkovic I. Matrix metalloproteinases in tumor invasion and metastasis. Semin Cancer Biol. 2000;10(6):415-33.

105.Leinonen T, Pirinen R, Bohm J, Johansson R, Kosma VM. Increased expression of matrix metalloproteinase-2 (MMP-2) predicts tumour recurrence and unfavourable outcome in non-small cell lung cancer. Histol Histopathol. 2008;23(6):693-700.

106.Hofmann HS, Bartling B, Simm A, Murray R, Aziz N, Hansen G, et al. Identification and classification of differentially expressed genes in non-small cell lung cancer by expression profiling on a global human 59.620-element oligonucleotide array. Oncol Rep. 2006;16(3):587-95.

107.Li M, Xiao T, Zhang Y, Feng L, Lin D, Liu Y, et al. Prognostic significance of matrix metalloproteinase-1 levels in peripheral plasma and tumour tissues of lung cancer patients. Lung Cancer. 2010;69(3):341-7.

108.Greenlee KJ, Werb Z, Kheradmand F. Matrix metalloproteinases in lung: multiple, multifarious, and multifaceted. Physiol Rev. 2007;87(1):69-98.

109.Kim SJ, Rabbani ZN, Dewhirst MW, Vujaskovic Z, Vollmer RT, Schreiber EG, et al. Expression of HIF-1alpha, CA IX, VEGF, and MMP-9 in surgically resected non-small cell lung cancer. Lung Cancer. 2005;49(3):325-35.

110.Leinonen T, Pirinen R, Bohm J, Johansson R, Ropponen K, Kosma VM. Expression of matrix metalloproteinases 7 and 9 in non-small cell lung cancer. Relation to clinicopathological factors, beta-catenin and prognosis. Lung Cancer. 2006;51(3):313-21.

111.Matsuyama M, Chijiwa T, Inoue Y, Abe Y, Nishi M, Miyazaki N, et al. Alternative splicing variant of vascular endothelial growth factor-A is a critical prognostic factor in non-small cell lung cancer. Oncol Rep. 2009;22(6):1407-13.

112.Shimanuki Y, Takahashi K, Cui R, Hori S, Takahashi F, Miyamoto H, et al. Role of serum vascular endothelial growth factor in the prediction of angiogenesis and prognosis for non-small cell lung cancer. Lung. 2005;183(1):29-42.

113.Takemoto N, Tada M, Hida Y, Asano T, Cheng S, Kuramae T, et al. Low expression of reversion-inducing cysteine-rich protein with Kazal motifs (RECK) indicates a shorter survival after resection in patients with adenocarcinoma of the lung. Lung Cancer. 2007;58(3):376-83.

114.Grossi F, Spizzo R, Bordo D, Cacitti V, Valent F, Rossetto C, et al. Prognostic stratification of stage IIIA pN2 non-small cell lung cancer by hierarchical clustering analysis of tissue microarray immunostaining data: an Alpe Adria Thoracic Oncology Multidisciplinary Group study (ATOM 014). J Thorac Oncol. 2010;5(9):1354-60.

115.Hoikkala S, Paakko P, Soini Y, Makitaro R, Kinnula V, Turpeenniemi-Hujanen T. Tissue MMP-2 and MMP-9 [corrected] are better prognostic factors than serum MMP-2/TIMP-2--complex or TIMP-1 [corrected] in stage [corrected] I-III lung carcinoma. Cancer Lett. 2006;236(1):125-32.

116.Martins SJ, Takagaki TY, Silva AG, Gallo CP, Silva FB, Capelozzi VL. Prognostic relevance of TTF-1 and MMP-9 expression in advanced lung adenocarcinoma. Lung Cancer. 2009;64(1):105-9.

117.Ylisirnio S, Hoyhtya M, Turpeenniemi-Hujanen T. Serum matrix metalloproteinases -2, -9 and tissue inhibitors of metalloproteinases -1, -2 in lung cancer--TIMP-1 as a prognostic marker. Anticancer Res. 2000;20(2B):1311-6.

118.Zheng S, Chang Y, Hodges KB, Sun Y, Ma X, Xue Y, et al. Expression of KISS1 and MMP-9 in non-small cell lung cancer and their relations to metastasis and survival. Anticancer Res. 2010;30(3):713-8.

119.Woo T, Okudela K, Yazawa T, Wada N, Ogawa N, Ishiwa N, et al. Prognostic value of KRAS mutations and Ki-67 expression in stage I lung adenocarcinomas. Lung Cancer. 2009;65(3):355-62.
120.Zhang SM, Zhu QG, Ding XX, Lin S, Zhao J, Guan L, et al. Prognostic value of EGFR and KRAS in resected non-small cell lung cancer: a systematic review and meta-analysis. Cancer Manag Res. 2018;10:3393-404.

121.Shi Y, Au JS, Thongprasert S, Srinivasan S, Tsai CM, Khoa MT, et al. A prospective, molecular epidemiology study of EGFR mutations in Asian patients with advanced non-small-cell lung cancer of adenocarcinoma histology (PIONEER). J Thorac Oncol. 2014;9(2):154-62.

122.Hirte H, Vergote IB, Jeffrey JR, Grimshaw RN, Coppieters S, Schwartz B, et al. A phase III randomized trial of BAY 12-9566 (tanomastat) as maintenance therapy in patients with advanced ovarian cancer responsive to primary surgery and paclitaxel/platinum containing chemotherapy: a National Cancer Institute of Canada Clinical Trials Group Study. Gynecol Oncol. 2006;102(2):300-8.

123.Bramhall SR, Schulz J, Nemunaitis J, Brown PD, Baillet M, Buckels JA. A double-blind placebo-controlled, randomised study comparing gemcitabine and marimastat with gemcitabine and placebo as first line therapy in patients with advanced pancreatic cancer. Br J Cancer. 2002;87(2):161-7.

124.Sparano JA, Bernardo P, Stephenson P, Gradishar WJ, Ingle JN, Zucker S, et al. Randomized phase III trial of marimastat versus placebo in patients with metastatic breast cancer who have responding or stable disease after first-line chemotherapy: Eastern Cooperative Oncology Group trial E2196. J Clin Oncol. 2004;22(23):4683-90.

125.Coussens LM, Fingleton B, Matrisian LM. Matrix metalloproteinase inhibitors and cancer: trials and tribulations. Science. 2002;295(5564):2387-92.

126.Winer A, Janosky M, Harrison B, Zhong J, Moussai D, Siyah P, et al. Inhibition of Breast Cancer Metastasis by Presurgical Treatment with an Oral Matrix Metalloproteinase Inhibitor: A Preclinical Proof-of-Principle Study. Mol Cancer Ther. 2016;15(10):2370-7.

127.Overall CM, Lopez-Otin C. Strategies for MMP inhibition in cancer: innovations for the post-trial era. Nature reviews Cancer. 2002;2(9):657-72.

128.Winer A, Adams S, Mignatti P. Matrix Metalloproteinase Inhibitors in Cancer Therapy: Turning Past Failures Into Future Successes. Mol Cancer Ther. 2018;17(6):1147-55.